



## Optimal routing of pedestrian flow in a complex topological network with multiple entrances and exits

Ruzelan Khalid, Mohd Kamal Mohd Nawawi, Luthful A. Kawsar, Noraida A. Ghani, Anton A. Kamil & Adli Mustafa

To cite this article: Ruzelan Khalid, Mohd Kamal Mohd Nawawi, Luthful A. Kawsar, Noraida A. Ghani, Anton A. Kamil & Adli Mustafa (2020) Optimal routing of pedestrian flow in a complex topological network with multiple entrances and exits, International Journal of Systems Science, 51:8, 1325-1352, DOI: [10.1080/00207721.2020.1756524](https://doi.org/10.1080/00207721.2020.1756524)

To link to this article: <https://doi.org/10.1080/00207721.2020.1756524>



Published online: 13 May 2020.



Submit your article to this journal [↗](#)



Article views: 256



View related articles [↗](#)








View Crossmark data [↗](#)



Citing articles: 1 View citing articles [↗](#)



## Optimal routing of pedestrian flow in a complex topological network with multiple entrances and exits

Ruzelan Khalid <sup>a</sup>, Mohd Kamal Mohd Nawawi <sup>a</sup>, Luthful A. Kawsar <sup>b,c</sup>, Noraida A. Ghani<sup>b</sup>, Anton A. Kamil <sup>d</sup> and Adli Mustafa <sup>e</sup>

<sup>a</sup>Institute of Strategic Industrial Decision Modeling, School of Quantitative Sciences, Universiti Utara Malaysia, Sintok, Malaysia; <sup>b</sup>School of Distance Education, Universiti Sains Malaysia, Penang, Malaysia; <sup>c</sup>Department of Statistics, School of Physical Sciences, Shahjalal University of Science and Technology, Sylhet, Bangladesh; <sup>d</sup>Faculty of Economics, Administrative and Social Sciences, Istanbul Gelisim University, Istanbul, Turkey; <sup>e</sup>School of Mathematical Sciences, Universiti Sains Malaysia, Penang, Malaysia

### ABSTRACT

A real-world topological network consists of multiple entrances along its source nodes. Routing appropriate percentages of pedestrians from these entrances to the particular available routes with relevant arrival rates will improve the network's performance. This paper presents a framework for finding the optimal arrival rates of pedestrians from all available entrances and routes to downstream nodes maximising the network's throughput. The calculation of the arrival rates and movement directions is based on *M/G/C/C* analytical and simulation models and the network flow model and considers the real distances of the entrances along the source nodes. The framework was tested on the Tuanku Syed Putra Hall, Universiti Sains Malaysia, Malaysia. Extensive analyses of the performances of its available nodes especially on the achievable optimal throughputs were documented and discussed. Quantitative results show that the hall's throughput is optimised when pedestrians' arrival rates to all the available entrances and their movement directions are controlled within certain ranges.

### ARTICLE HISTORY

Received 30 September 2019  
Accepted 12 April 2020

### KEYWORDS

*M/G/C/C*; network flow model; simulation; facilities planning and design; queuing networks

## 1. Introduction

Many buildings and transportation networks now implement evacuation plans and route assignments to reduce the risks of injury or death during emergency cases; e.g. fire and bomb threat. Conventional plans simply recommend that occupants use the safest, shortest or even easiest exit routes along their movement. Such movement is also a typical approach considered by human natural psychology and behaviour during emergency cases. However, the approach may not be the best evacuation strategy. For example, if all occupants use their shortest routes without any proper control during high loads, the routes will then be over utilised after a certain point of time. This situation will create unsteady flow which can cause congestion along the travel routes, block incoming pedestrians and eventually decrease the overall evacuation performance (Gao et al., 2014; Shende, 2008; Stepanov & Smith, 2009).

The stability of flow in a topological network significantly depends on its traffic loads; i.e. the number of pedestrians in all its available routes. Each route has its own capacity to support the intense demand of pedestrians. Any increase in the number of residing pedestrians will decrease the current walking speed and reduce the overall flow in the network. To avoid the over utilisation, the flow in the network should be analysed and optimised. For this, various scientific approaches combining different fields of knowledge (e.g. operations research, computer science and transportation engineering) and striving to model what may actually happen during pedestrian flow have been proposed. The approaches include the use of integer programming to design and analyse network routes (Stepanov & Smith, 2009), mixed integer programming to reduce delays and improve traffic flow at intersections (Cova & Johnson, 2003) and the ant colony algorithm to determine the optimal route to best flow

occupants from a facility (Fang, Zong, et al., 2011). In fact, facilities with complex network topologies have made pedestrian flow analyses significantly important. However, most of the flow analyses focused by previous research have only revolved around identifying the potential bottlenecks at particular networks or determining the impacts of operational policies on the current and alternative physical designs (e.g. Cruz et al., 2005, 2010, 2012; Cruz & Smith, 2007; Hu et al., 2015; Huang et al., 2018; Jiang et al., 2016; Khattak et al., 2017, 2018; van Woensel & Cruz, 2014; Zhu et al., 2017). Other research (e.g. Cuesta et al., 2017; Saeed Osman & Ram, 2017; Taneja & Bolia, 2018) meanwhile optimised the flow in a topological network based on the optimal network routes without optimising both of pedestrian arrival rates to all its available entrances (i.e. the arrival sources where pedestrians start walking) and routing probabilities (i.e. their movement directions) to relevant downstream nodes (individual networks). It is thus important to derive the optimal arrival rates and routing probabilities maximising the overall throughput of a topological network with small blocking probabilities along all its routes.

The objective of this paper is to derive pedestrians' optimal arrival rates to all available entrances and their movement directions maximising the overall flow in a complex topological network using an  $M/G/C/C$  state-dependent queuing model (Cheah & Smith, 1994; Cruz et al., 2005; Cruz & Smith, 2007; Jain & Smith, 1997; Smith & Cruz, 2014; Weiss et al., 2012) and a network flow model. A network flow model and its variation models are a common tool used in previous studies (e.g. Cova & Johnson, 2003; Farahani et al., 2018; Kimms & Maiwald, 2017) for investigating movement or evacuation planning. How to set the parameters and constraints of the network flow model using  $M/G/C/C$  is the main interest of this paper.  $M/G/C/C$  is used to analyse and simulate pedestrians' travel behaviours and find the optimal arrival rate to each node maximising its throughput while minimising its blocking probability. The optimal arrival rates of all nodes are then set as the flow capacity constraints of the network flow model whose objective is to find the optimal arrival rates to the available entrances and movement directions to relevant exits maximising the overall flow in the topological network. As a case study, we consider a network of corridors in the Tuanku Syed Putra Hall (DTSP), Universiti Sains Malaysia, Malaysia.

The derivation of the optimal arrival rates to source nodes based on an analytical  $M/G/C/C$  model and a network flow model has actually been discussed in R. Khalid, Baten, et al. (2016). They, however, assume that each source node only has a single arrival source located at its origin. In reality, a source node typically has multiple entrances along with it. How pedestrians move from the entrances to their available downstream nodes will definitely determine the overall throughput of the network. However, the effect of such movement directions on the throughput was not considered in their paper. Additionally, how the analytical throughput matches the throughput of a simulation model and how sensitive the throughput to the changes in arrival rates was also not discussed. This paper thus offers two main contributions. The first contribution is the proposal of a framework for deriving pedestrians' optimal arrival rates and movement directions in a network with multiple entrances and exits based on the combination of  $M/G/C/C$  and network flow models. The framework helps decision makers find strategies to optimally flow pedestrians to their downstream nodes in a complex topological network. The second contribution is the extensive quantitative analysis of pedestrian flow in a network based on analytical and simulation models. The analysis helps decision makers get insight into the effect of arrival rates and movement directions on the performance of a network in terms of its blocking and throughput and how the performance can be optimised by controlling both of the arrival rates and movement directions within certain ranges.

This paper is structured as follows. Section 2 briefly collects some literature reviews related to this study. In Section 3, we briefly discuss a framework for optimising the flow in a topological network with multiple entrances and exits using the  $M/G/C/C$  and network flow models. The framework derives the optimal arrival rates and pedestrian movement directions in the network. How sensitive the arrival rates to the performance of the network are also discussed. Section 4 utilises the framework to flow pedestrians in a network based on relevant routing policies, considering the DTSP as a case study. The performance of the policies including the optimal policy using the optimal arrival rates and routing strategies based on  $M/G/C/C$  analytical and simulation models is presented in Section 5. In this section, we also propose some recommendations for optimising pedestrians' flow in the hall. Finally,

Section 6 summarises the findings and presents some conclusions.

## 2. Literature review

Pedestrian movement in a network is influenced by various travel characteristics such as walking speed and different routing patterns. The walking speed has been argued (e.g. by Cao et al., 2017; Drake et al., 1965; Drew, 1968; Greenberg, 1959; Greenshields, 1935; Hänseler et al., 2017; Hu et al., 2015; Jiang et al., 2016; Pipes, 1967; Underwood, 1960; Yuhaski & Smith, 1989) to be dependent on pedestrian density in each node decreasing with the increased density of the pedestrians. The density is sequentially affected by the incoming pedestrians from its upstream nodes. The density can be controlled to improve the flow in all routes by managing the pedestrians' arrival to all available entrances and their movement directions to relevant downstream nodes.

In emergency situations, such movement becomes more complicated since pedestrians are typically nervous and panic. These feelings can ignite unpredictable behaviour such as stampede, trampling and pushing which significantly delays their movement and causes havoc along the movement routes. The behaviour is very complex and difficult to capture in mathematical equations or computer simulation (Helbing et al., 2002; Peacock et al., 2011). This difficulty has imposed many studies to only derive the best or optimal movement in a normal situation (i.e. a state where pedestrians are in rational normal behaviour) using relevant approaches; e.g. flow-based modelling (Asano et al., 2007; Fang, Li, et al., 2011; Hänseler et al., 2004; Hughes, 2002; Zhang et al., 2016), cellular automata (Blue & Adler, 2001; Burstedde et al., 2001; Sarmady et al., 2011; Zhang et al., 2017) and multi-agent based systems (Antonini et al., 2006; Hernández et al., 2011).

The flow-based modelling approach has long been used to model the evacuation of evacuees from a large scale topological network or the flow of pedestrians in a complex topological facility building. In this case, designing the optimal evacuation routes is necessary for minimising the total clearance time of the network. The routes are typically derived using relevant operations research methods; e.g. linear programming, mixed integer linear programming, simulation-based assessment or heuristics embedding with a relevant density-flow model or integrating with an available

traffic simulation package for modelling the dynamic of traffic flow. Some studies focusing on transporting evacuees from area to area in a large network include Murray-Tuite and Mahmassani (2003), Sayyady and Eksioglu (2010), Chen and Chou (2009), Naghawi and Wolshon (2012), Campos et al. (2012) and Kunwar et al. (2016).

There have also been studies focusing on building or facility evacuation. Chalmet et al. (1982), for example, developed a model determining evacuation routes of a complex structure multi-story building. For each route, its evacuation status especially the time to evacuate occupants was calculated using their arrival rates to the source nodes (e.g. halls and lobbies) and the capacity of confined spaces (e.g. stairwells). To find the ideal number of occupants to use each available exit route minimising the total clearance time, Pursals and Garzón (2009) formulated an advanced flow model. The model replicates the effect of occupants' density on their speed in a space. How pedestrian dynamics movements in a space are effected by different age compositions were investigated by Cao et al. (2016). The effect of other relevant properties; e.g. visibility and occupant types on pedestrian evacuation in a room were meanwhile considered by Cao et al. (2015, 2018) in their multi-grid model. Additionally, an efficient flow and evacuation approach to achieve the target evacuation time during mass gathering from source to sink nodes by utilising their available capacities was proposed by Taneja and Bolia (2018). M. N. A. Khalid and Yusof (2018), as another example, combined crowd modelling techniques and flexible routing approach to measure pedestrian evacuation plan performance. Meanwhile, the effect of pedestrian density on the uni-, bi- and multi-directional flow within facilities was captured by Smith (1991) in an *M/G/C/C* model. In the meantime, various computer evacuation models with their features (e.g. modelling methods and visual simulation support) and limitations (e.g. processing time and model capacity) to simulate the crowd movement in buildings have also been discussed and reviewed (e.g. Gwynne et al., 1999; Kuligowski et al., 2005).

*M/G/C/C* measures network performance in terms of the throughput, blocking probability, expected number of entities and expected service time. To maximise the throughput, previous studies (e.g. Smith & Kerbache, 2011; Stepanov & Smith, 2009) utilised

*M/G/C/C* to find the optimal routing policy or analyse the effect of arrival rates of entities to source networks. The importance of controlling arrival rates to achieve a better throughput has also been argued in many other studies (Cheah & Smith, 1994; Cruz et al., 2005; Cruz & Smith, 2007; Kawsar et al., 2013; Smith, 2012; Weiss et al., 2012; Yuhaski & Smith, 1989). Cruz et al. (2005), for example, developed an *M/G/C/C* analytical model for a ten-story building and found that the throughput at the ground floor was significantly influenced by the arrival rate to each of its stairwells. To validate the analytical results, Cruz and Smith (2007) developed its counterpart *M/G/C/C* simulation model and then compared the results generated by both models. The results showed that both models generated almost similar performance measures.

Coding *M/G/C/C* libraries for simulating pedestrians' dynamic behaviour using object-oriented programming languages, e.g. Java (Garrido, 2001) and C++ (Garrido, 1998) is time-consuming and difficult. To cater this, R. Khalid et al. (2013) discussed how Arena (Kelton et al., 2015) can simulate the effects of arrival rates on the performance of a network (node). Arena itself is not designed to directly handle the state-dependent service rates instantaneously altered as a function of the number of pedestrians as they flow in the node. The service rates can, however, be programmed using Arena's special available modules. For a source node consisting of multiple entrances with their own distances to the end of the node, R. Khalid, Nawawi, et al. (2016) studied the effect of treating the entrances as a single source on the performance of the node using *M/G/C/C* weighted distance and real distance simulation models. Unfortunately, no optimal arrival rates and movement directions were discussed.

Arrival rates maximising the throughputs of source nodes may not maximise the throughputs of their downstream nodes since the rates could create blockings along the node links. The same concept also applies to travel routes. The shortest route believed to be the fastest way of flowing pedestrians may overexploit the downstream nodes and cause massive congestion along the node links (Stepanov & Smith, 2009). Minimising the congestion by controlling the arrival rates to available entrances and appropriately routing pedestrians to downstream nodes especially during emergency cases is thus crucial.

### 3. Framework of optimising pedestrian flow in a complex topological network with multiple entrances

#### 3.1. Framework assumptions

Our framework only considers a space size and its current number of pedestrians in modelling the flow behaviour as replicated by an *M/G/C/C* model. This model ignores pedestrians' attributes (e.g. gender, age, personality, mood and body size) and other environmental factors (e.g. floor material and lighting levels) in spite of the fact that they can actually influence their movement in a circulation space. However, the attributes and environmental factors have trivial effect on the movement when the traffic density increases (Mitchell & Smith, 2001). Additionally, our framework derives the optimal flow of pedestrians in a topological network in a normal situation. Under this situation, human complex and unpredictable behaviour over time during emergency situations (e.g. panic, confusion and loss of orientation) creating unexpected patterns of movement (e.g. stumbling, herding and flocking) and reducing pedestrian flow in the network has been ignored. Ignoring this aspect enables us to model pedestrian dynamic movement using analytical and simulation models. Both models can then be used to evaluate and assess various determined strategies.

Pedestrians are assumed to start travelling from all entrance sources and move freely without any obstacles through the network or blockages in their exits. Any obstacles or blocked exits reduce the optimal flow. To optimise the flow, all available paths are analysed based on their flow capacities. The capacities are used to find the optimal arrival rates to entrances and movement paths from the arrival to exit sources. We further assume that arrival rates can be controlled to meet their optimal flow rates.

#### 3.2. Finding the optimal arrival rate of an *M/G/C/C* network

*M/G/C/C* models the arrival of pedestrians at a network (according to the *Markovian* process) and their flow with relevant speed variably changed based on the current density of residing pedestrians. The *M/G/C/C* model was originally based on Tregenza's curves (Tregenza, 1976). The data of the curves were retrieved from some previous empirical studies (e.g. Foot, 1973; Hankin & Wright, 1958; Togawa, 1955). How the

arrival rate affects the flow performance based on mathematical equations has been documented in previous studies (e.g. Cruz et al., 2005; Cruz & Smith, 2007; Mitchell & Smith, 2001; Smith, 2001; Smith & Cruz, 2014; Weiss et al., 2012; Yuhaski & Smith, 1989). Its mathematical equations are as follows:

$$V_n = V_1 \exp \left[ - \left( \frac{n-1}{\beta} \right)^\gamma \right] \quad (1)$$

where

$$\gamma = \frac{\ln \left[ \frac{\ln(V_a/V_1)}{\ln(V_b/V_1)} \right]}{\ln \left( \frac{a-1}{b-1} \right)},$$

$$\beta = \frac{a-1}{\left[ \ln \left( \frac{V_1}{V_a} \right) \right]^{1/\gamma}} = \frac{b-1}{\left[ \ln \left( \frac{V_1}{V_b} \right) \right]^{1/\gamma}},$$

$\gamma$ ,  $\beta$  = shape and scale parameters for the exponential model,  $V_n$  = average walking speed for  $n$  pedestrians in the network,  $V_a$  = average walking speed when crowd density is 2 peds/m<sup>2</sup> = 0.64 m/s,  $V_b$  = average walking speed when crowd density is 4 peds/m<sup>2</sup> = 0.25 m/s,  $V_1$  = average walking speed for a single pedestrian = 1.5 m/s,  $n$  = number of pedestrians in the network,  $a = 2 \times L \times W$ ,  $b = 4 \times L \times W$ ,  $L$  = network length in metres, and  $W$  = network width in metres.

The model can also approximate the walking speed for bi-directional and multi-directional flow by changing the parameter values of  $V_a$  and  $V_b$  (Cheah, 1990; Cheah & Smith, 1994). For bi-directional flow,  $V_a = 0.60$  m/s and  $V_b = 0.21$  m/s while for multi-directional flow,  $V_a = 0.56$  m/s and  $V_b = 0.17$  m/s. Using the speed-density relationship, the performance of a network can be measured as:

$$\theta = \lambda(1 - P_{block}), E(N) = \sum_{n=1}^C nP_n \text{ and } E(T) = \frac{E(N)}{\theta} \quad (2)$$

$\lambda$  is the arrival rate to the network; i.e. the number of pedestrians arriving to the network in a second (peds/s).  $\theta$  is the throughput of the network; i.e. the number of pedestrians exiting the network in a second (peds/s).  $E(N)$  is the expected number of pedestrians residing in the network (peds).  $E(T)$  is the expected service time; i.e. the travel time spent by pedestrians exiting the network (seconds).  $C$  is the capacity of the network; i.e. the available space to accommodate

pedestrians which is  $5 \times L \times W$ .  $P_{block}$  is the blocking probability of the network (i.e. the probability that arriving pedestrians are blocked from entering the network because of its available spaces are being used by other pedestrians) whose situation occurs when  $P_n = C$ .  $P_n$  is the probability when there are  $n$  pedestrians in the corridor and is given by

$$P_n = \frac{[\lambda E(S)]^n}{n!f(n)f(n-1) \dots f(2)f(1)} P_0 \quad (3)$$

$$n = 1, 2, 3, \dots, C$$

where,

$$P_0^{-1} = 1 + \sum_{n=1}^C \left[ \frac{[\lambda E(S)]^i}{i!f(i)f(i-1) \dots f(2)f(1)} \right].$$

$E(S)$  is the expected service time of a single pedestrian in the network given by  $E(S) = L/1.5$  where  $L$  is the average travel distance,  $P_0$  is the probability when there is no pedestrian in the network, and  $f(n)$  is the service rate and given by  $f(n) = V_n/V_1$ .  $V_n$  is the current pedestrian speed in the network as given in Equation (1).

An arrival rate is one of the input parameters for the M/G/C/C model. By letting the other input parameters; i.e. the length, width and pedestrian travel distance of a network be constant, its optimal arrival rate can then be derived. How to derive the optimal arrival rate using calculus and numerical analysis has been discussed in R. Khalid, Baten, et al. (2016). This static performance approximation can be validated using simulation. We chose Arena to simulate the M/G/C/C logic for two reasons. First, it provides Process Analyzer, a user-friendly platform to report the effects of arrival rates on a network's performance. Second, it provides OptQuest to search the optimal arrival rate subject to relevant constraints. To confine the search, the arrival rate should have lower and upper values as its bound, and a suggested value as its initial searching point. To set the bound, the suggested value is initially fed with the optimal arrival rate based on its analytical model.

The suggested value is then decreased by 10% to be the lower bound and increased 10% to be the upper bound. The throughputs at the near end of the lower and upper bounds and the highest throughput generated by OptQuest are then observed. If the highest throughput occurs at the near lower bound, the range is to be adjusted to the left side with the new suggested value is the lower bound value. Similarly, if the highest

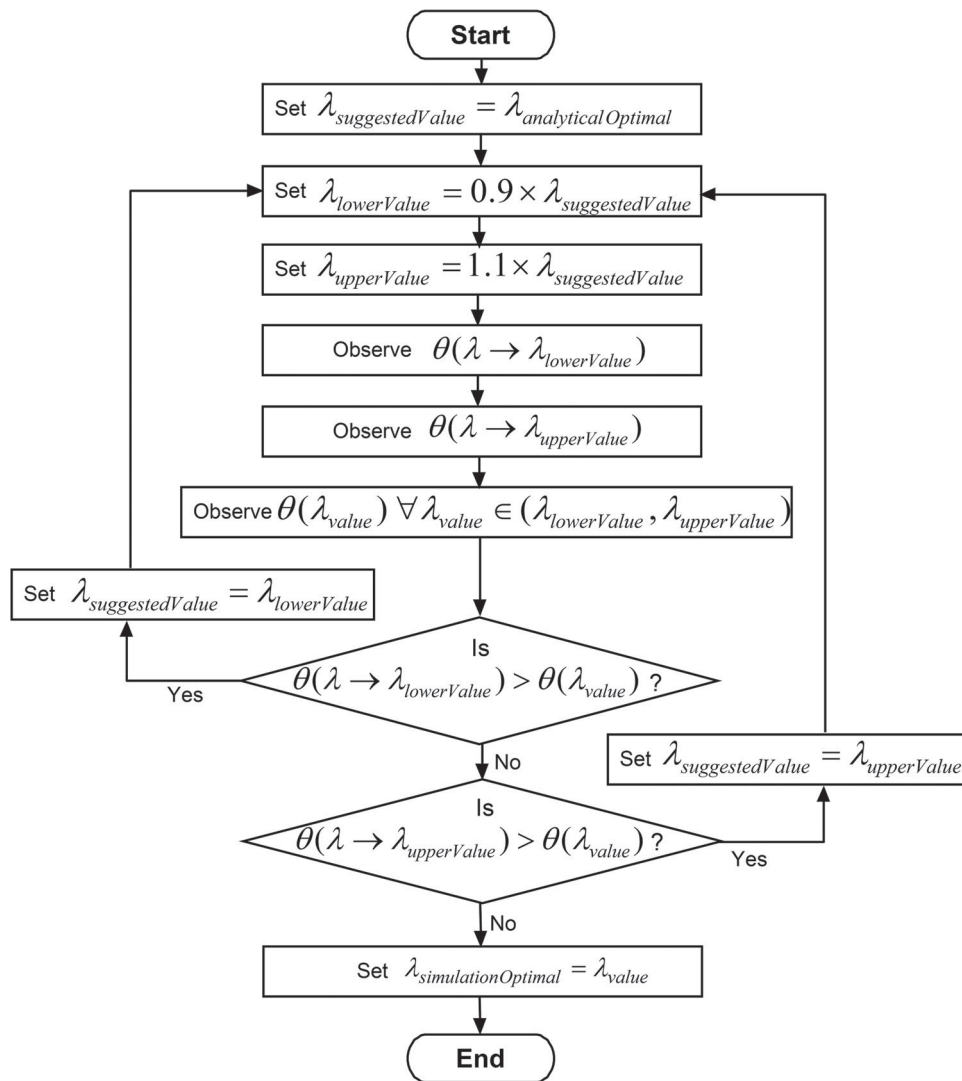


**Figure 1.** Finding the optimal arrival rate based on simulation.

throughput occurs at the near upper bound, the range is to be adjusted to the right side where the new suggested value is the upper bound value. This process is repeated until the three throughput values show the concave pattern. In this case, the arrival rate generating the highest throughput is the optimal arrival rate. The process of finding the lower and upper bounds and the optimal arrival rate based on simulation is illustrated in Figure 1. In the figure,  $\lambda$  refers to the arrival rate while  $\theta$  refers to the throughput.

### 3.3. Optimising the flow in an M/G/C/C topological network

A complex network is structured by many source, intermediate and sink (exit) nodes. In real-life systems, a node represents a segment of corridors, roads or

spaces with a particular size of length and width (Cruz & Smith, 2007; Mitchell & Smith, 2001; Smith, 2011). The nodes are linked to each other to form a topological network where flow can occur. The flow starts from the source nodes; i.e. the entryway nodes where entities (e.g. pedestrians and vehicles) in a unit of time arrive and flow from node to node through available links.

The links between nodes form three types of topologies; i.e. series, splitting and merging topologies. How these topologies are extracted from a system are illustrated in Figure 2. For each topology, the flow conservation (Kachroo, 2009; Kachroo et al., 2008; Shende, 2008) and the flow capacity of its nodes limiting the amount of flow to the nodes must be satisfied. For example, the flow conservation in a series topology formed by node 1, node 2 and node 3 (see Figure 1) is

given by  $x_{1 \rightarrow 2} = x_{2 \rightarrow 3}$  where  $x_{i \rightarrow j}$  represents the flow from node  $i$  to node  $j$ .

The network we consider has multiple sources ( $s_1, s_2, \dots, s_n$ ) and sinks ( $t_1, t_2, \dots, t_n$ ). This network has to be converted to a network having a unique source and sink by creating a fictitious super-source  $S$  and a fictitious super-sink  $T$ . The flow capacities (i.e. the maximum number of pedestrians per unit time that can flow) from the super-source  $S$  into each available source ( $S, s_i$ ) and the flow capacities from the super-sink  $T$  into each available sink ( $t_j, T$ ) are unlimited; i.e.  $c(S, s_i) = c(t_j, T) = \infty$ . The optimal flow from the super-source  $S$  to the super-sink  $T$  (the optimal flow in the network) can be modelled as a linear program as follows:

#### Notation

$i$  = an index for origin node  $i$  ( $i = 1, 2, \dots, n$ ) of a set of origin nodes,  $I$ .

$j$  = an index for destination node  $j$  ( $j = 1, 2, \dots, n$ ) of a set of destination nodes,  $J$ .

#### Decision variable

$x_{i \rightarrow j}$  = the flow from origin node  $i$  to destination node  $j$ .

#### Mathematical formulation

Maximise $x_{T \rightarrow S}$	$x_{T \rightarrow S}$ represents the flow from super-sink node $T$ back to super-source node $S$
subject to:	
$\sum_j x_{S \rightarrow j} - x_{T \rightarrow S} = 0$	outflow of super-source node $S$ to its downstream nodes must be equal to inflow from super-sink node $T$
$\sum_j x_{i \rightarrow j} - (x_{S \rightarrow i} + \sum_j x_{j \rightarrow i}) = 0$	outflow of source node $i$ ( $i = s_1, s_2, \dots, s_n$ ) to its downstream nodes must be equal to inflow from super source $S$ and inflow from its upstream nodes (in case the source node is also an intermediate node)
$\sum_j x_{i \rightarrow j} - \sum_j x_{j \rightarrow i} = 0$	outflow of node $i$ to its downstream nodes must be equal to inflow from its upstream nodes for every node $i \neq s, t$
$(x_{i \rightarrow T} + \sum_j x_{i \rightarrow j}) - \sum_j x_{j \rightarrow i} = 0$	outflow of sink node $i$ ( $i = t_1, t_2, \dots, t_n$ ) to super node $T$ and outflow to its downstream nodes (in case the sink node is also an intermediate node) must be equal to its inflow from upstream nodes
$x_{T \rightarrow S} - \sum_j x_{j \rightarrow T} = 0$	outflow of super-sink node $T$ to super-source node $S$ must be equal to inflow from its upstream nodes
$\sum_j x_{j \rightarrow i} \leq \lambda_{optimal_i}$	total inflow capacity to every node $i$ must be smaller or equal to its optimal arrival rate
$x_{i \rightarrow j} \geq 0$	flow for every node $i$ to node $j$ must be non-negative

Note that the decision variable is a discrete variable modelling the movement of individual pedestrians. The movement process continues from node to node where the total throughput of the upstream nodes (in pedestrians/second) will be the arrival for the downstream nodes. How flow is conserved between nodes and controlled to avoid blockages can be modelled using the network flow model.

This model finds the optimal flow through the network with multiple sources and sinks. As observed, optimising arrival rates to source nodes and flow to other nodes requires the network to be decomposed into individual independent nodes. These nodes are to be analysed separately. However, the network is a finite capacity topological network where each node is state dependent. Since state dependent nodes are finite, treating the nodes as separate individual nodes will explicitly ignore blockages which may happen in the network during the flow processes. How to avoid this situation?

Our strategy is to minimise the blocking probability of each node to avoid any blockages between the node links while maximising its flow. Pedestrians should thus be flowed to a relevant node up to its optimal arrival rate. For this, the total flow to the node must be smaller or equal to its optimal arrival rate to minimise any blockage. This condition is satisfied by setting the optimal arrival rate as the inflow capacity to the node; i.e.  $\sum_j x_{j \rightarrow i} \leq \lambda_{optimal_i}$  where  $\lambda_{optimal_i}$  is a parameter; i.e. the optimal arrival rate to node  $i$  whose value is determined by the capacity of the node. The optimal arrival rate of each node based on the analytical model can be derived using the formula discussed in R. Khalid, Baten, et al. (2016) while the optimal arrival rate of the node based on the simulation model is derived using OptQuest. If the capacities of two nodes are equal, then the node with a shorter distance will definitely have a bigger optimal flow. The outflow of the node must also be equal to its inflow; i.e.  $\sum_j x_{i \rightarrow j} - \sum_j x_{j \rightarrow i} = 0$ . Additionally, all flow has to be non-negative; i.e.  $x_{i \rightarrow j} \geq 0$ .

There are to be two network flow models. The first model uses the optimal arrival rates of all nodes based on the analytical model. The second model uses the optimal arrival rates of all nodes based on the simulation model.



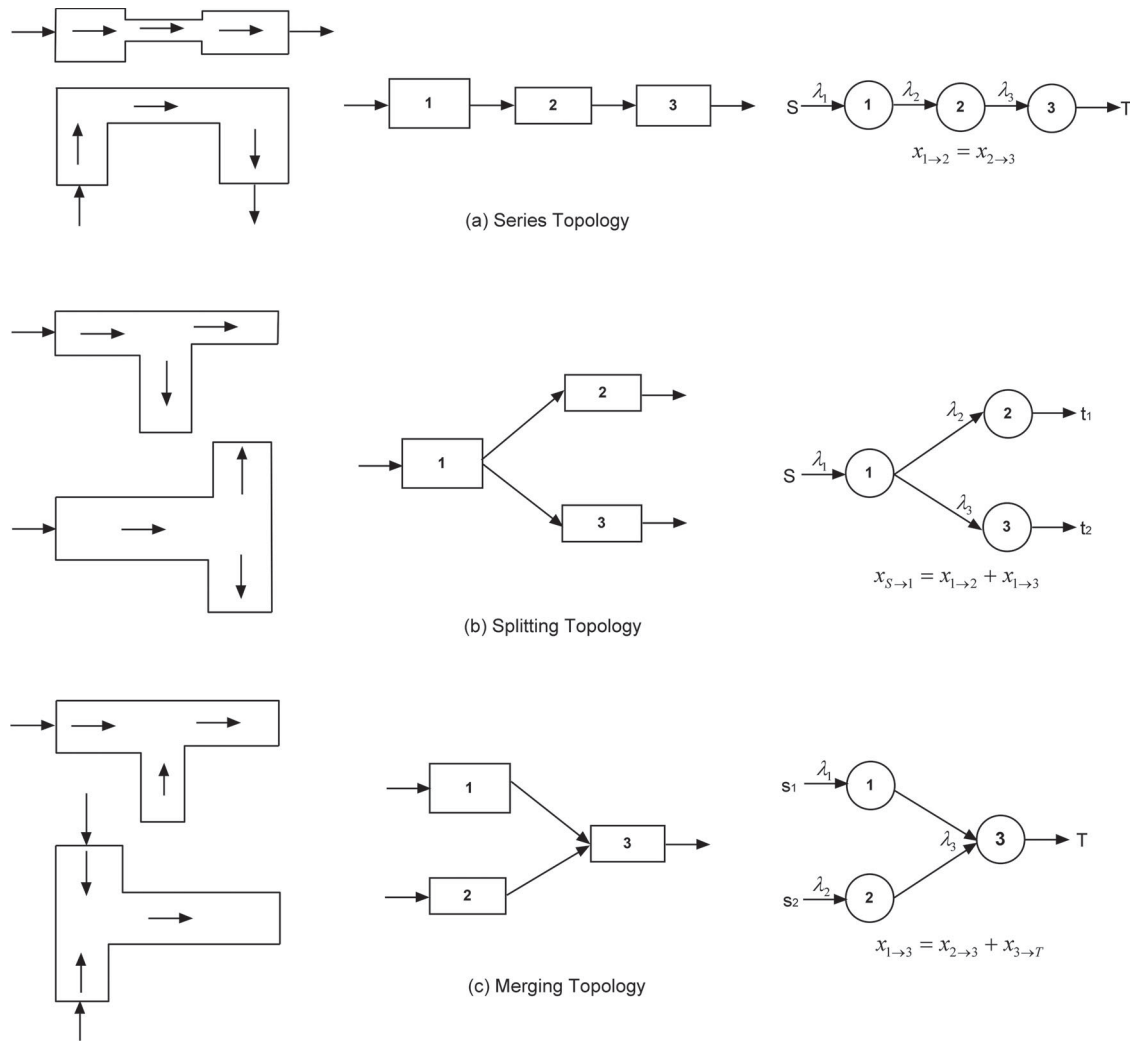


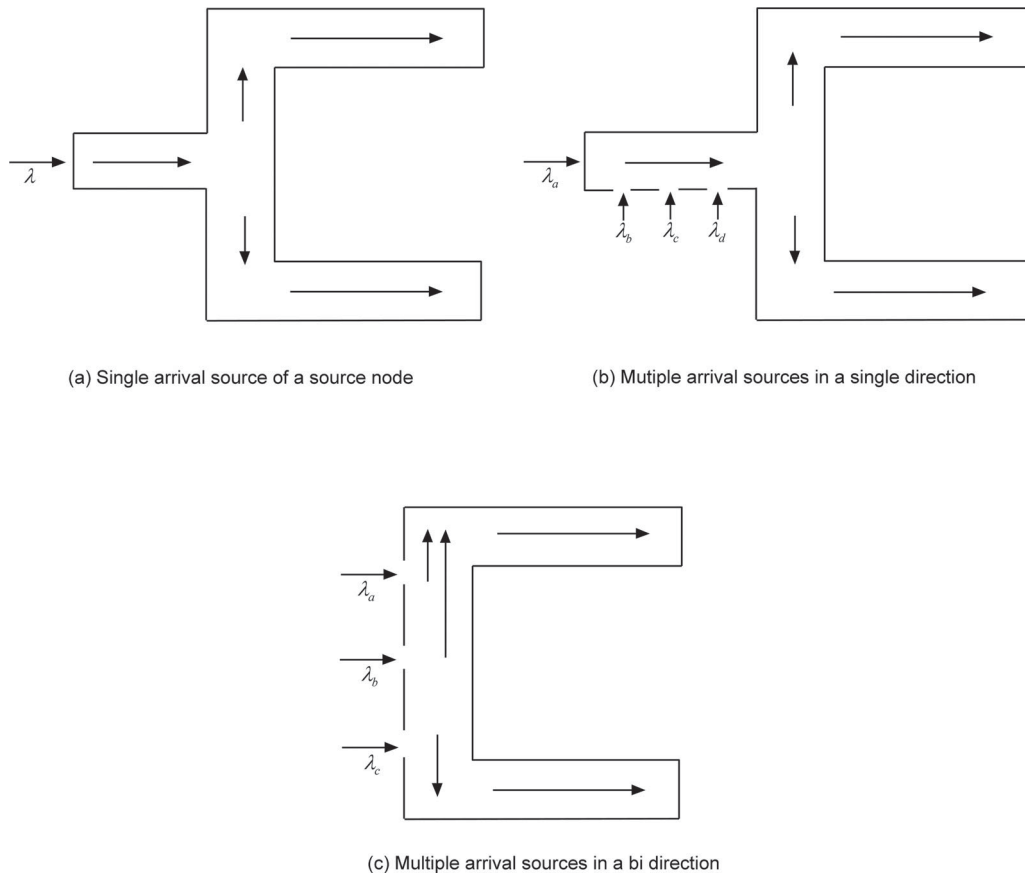
Figure 2. Conversion of various physical topological networks.

**3.4. Optimising the flow in a source node with multiple entrances**

A topological network may consist of many source nodes. A source node is the first node entered by pedestrians before travelling to downstream nodes. It can be of two cases. In a simple case, it only has a single entrance located at its origin (Figure 3(a)). An example of this is a single-entry traffic corridor. As intermediate or sink nodes, the pedestrians’ average travel distance is simply the length of the node. In a more complex case, the source node has multiple entrance scattered at various locations along it (Figure 3(b or c)). A typical example of this is a complex subway station. In the station, there may be some confined spaces with multiple entrances allowing pedestrians to enter the spaces from various angles before travelling to other spaces. Based on this concept, a single-entrance node is thus a subset or a special case of a multi-entrance node.

The distances from each of the entrances to the end of the node differ from each other. These various distances can be attached to the attribute of pedestrians in the simulation model. However, the distances have to be averaged before being set in the analytical model since it can only accept the weighted distance travelled by all pedestrians. To find this weighted distance, the node has to be converted to a single equivalent node. Assume that the node has  $k$  entrances with arrival rates of  $\lambda_1, \lambda_2, \dots, \lambda_k$  whose travel distances to the end of the node are  $L_1, L_2, \dots, L_k$  respectively. Based on the work of Yuhaski and Smith (1989), the node can be modelled as another single node of length  $L'$  and arrival rate  $\lambda'$  such that

$$\lambda' = \sum_{i=1}^k \lambda_i \text{ and } L' = \frac{\sum_{i=1}^k \lambda_i L_i}{\sum_{i=1}^k \lambda_i} \tag{3}$$



(a) Single arrival source of a source node

(b) Multiple arrival sources in a single direction

(c) Multiple arrival sources in a bi direction

**Figure 3.** Multiple entrances of a source node.

In Equation (3),  $L'$  is the weighted distance travelled by all the arrivals of  $\lambda_1, \lambda_2, \dots, \lambda_k$ . If we further assume that  $\lambda_1 = \lambda_2 = \dots = \lambda_k$ , then

$$L' = \frac{\lambda \sum_{i=1}^k L_i}{k\lambda} = \frac{\sum_{i=1}^k L_i}{k} \quad (4)$$

Equation (4) calculates the weighted distance travelled by pedestrians from multiple entrances along a source node for single (Figure 3(b)) or bi-direction (Figure 3(c)) flow. The percentage or probability flow to the ends of the node determines the weighted distance. For example, consider that node 2 is a source node connected with node 5 in its left and node 6 in its right, and has  $k$  entrances along it. The number of pedestrians travelling to nodes 5 and 6 will affect the probability of pedestrian flow from node 2 and their weighted distance. For example, assume that  $k=3$  and  $L_{2,i \rightarrow j}$  represents the distance of arrival source  $i$  in node 2 to node  $j$ . If 50% of pedestrians from the first entrance (source 1) are directed to travel to node 5 while the other pedestrians from sources 2 and 3 are directed to travel to node 6, then the routing probability of node 2 is  $1/6$ . For this probability, the weighted travel distance

of node 2 is  $L'_2 = \frac{0.5L_{2,1 \rightarrow 5} + 0.5L_{2,1 \rightarrow 6} + L_{2,2 \rightarrow 6} + L_{2,3 \rightarrow 6}}{3}$ . If the probability is set to 0.5, all pedestrians from source 1 and 50% of pedestrians from source 2 then have to travel to node 5 while the other pedestrians have to travel to node 6. The weighted travel distance of node 2 is then  $L'_2 = \frac{L_{2,1 \rightarrow 5} + 0.5L_{2,2 \rightarrow 5} + 0.5L_{2,2 \rightarrow 6} + L_{2,3 \rightarrow 6}}{3}$ . If the probability is set to 1, all pedestrians from these three entrances have to travel to node 5. The weighted travel distance of node 2 is then  $L'_2 = \frac{L_{2,1 \rightarrow 5} + L_{2,2 \rightarrow 5} + L_{2,3 \rightarrow 5}}{3}$ .

In simulation, the probability can be set using a decision module. The module should follow each entity creation module representing an entrance of pedestrians. The general expression for flowing pedestrians from a source node with a number of entrances to relevant directions is as follows:

$$\text{Decision}_i = \min(\max(\text{Total Number Of Entrances} \\ * P_{\text{Source Node} - (i-1), 0}, 1)$$

For example, the expression for the decision module following the first entrance of node 2 is  $\min(\max(3 * P_2, 0), 1)$ . If  $P_2 \geq 2/6$ , then all pedestrians from its entrance 1 will travel to the right; i.e. node 6. As

other examples, imagine that node 10 has 10 entrances while node 11 has 8 entrances. Thus, the expression of the decision module for entrance 3 of node 10 is  $\min(\max(10 * P_{10} - 2, 0), 1)$  while that for entrance 7 of node 11 is  $\min(\max(8 * P_{11} - 6, 0), 1)$ . The probability values should be stored in a variable so that it can flexibly be adjusted to accommodate the routing probability.

### 3.5. Finding the optimal arrival rates and routing probabilities of source nodes

Our objective is to derive the optimal arrival rates to source nodes and routing probabilities to downstream nodes. Without the optimal routing probabilities, the weighted travel distance of the source node for the analytical model cannot be computed. Consequently, this prohibits the calculation of its optimal arrival rate. To handle the problem, we initially set the default routing probability for each source node. For this, we assume that its optimal routing probability is 0.5. This assumption enables us to find its optimal arrival rate using the analytical and simulation models. For analytical, we first calculate its weighted travel distance based on this strategy. Using the distance and the capacity, its optimal arrival rate can then be calculated. For simulation, we first set the distance of each of its entrances and then set its flow probability to 0.5 (i.e.  $P_{\text{SourceNode}} = 0.5$ ). Its optimal arrival rate is then searched using OptQuest.

All individual nodes' optimal arrival rates based on analytical and simulation are separately set as the flow constraints of the network flow model. Both models are then solved to find the optimal flows to the source nodes maximising the whole network's flow. Using the optimal flows, we then calculate the optimal pedestrian routing probability of each source node to both of its ends. For example, assume that the network flow model reports that  $x_{S \rightarrow 2} = \alpha$  maximises the flow with the conditions that  $x_{2 \rightarrow 5} = \beta$  ( $\beta \leq \alpha$ ) and  $x_{2 \rightarrow 6} = \alpha - \beta$ . Based on these values, the optimal routing probability from node 2 to its downstream nodes can then be calculated. Of pedestrians in node 2,  $(\beta/\alpha) \times 100$  should be routed to node 5 while the remaining  $((\alpha - \beta)/\alpha) \times 100$  to node 6. Since node 2 has  $k$  entrances, pedestrians from the first  $(\beta/\alpha) \times k$  of the entrances should travel to the left while  $1 - ((\beta/\alpha) \times k)$  should travel to the right.

The optimal routing probability value can directly be set in the simulation model. In this case,  $P_2 = \beta/\alpha$ . Based on this probability, we once again use OptQuest to find its optimal arrival rate under the optimal routing based on simulation. For the analytical model, the probability value is used to calculate the weighted travel distance of pedestrians in node 2 to node 5 or/and node 6. The distance is then used to find the optimal arrival rate of node 2 under the optimal routing. Since the capacity of node 2 stays constant, this new optimal arrival rate value for both models should be smaller than that of the default strategy for any increment in the weighted travel distance and vice versa. The new optimal arrival rate is then compared to the lower and upper bounds of the optimal flow of the default strategy generated while performing the sensitivity analysis of the model. This post-optimality analysis measures the sensitivity of any changes of the arrival rate of each source node to the whole network's flow. The impact can be of two cases.

The first case is the new optimal arrival rate is within an allowable range. Its impact can directly be measured by looking at its slack variable and dual price value without the need to re-solve the network flow model. For any source node, the dual price of 0.0000 indicates that any increment or decrement in its arrival rate within an allowable range will not change the current solution since it still has an unused inflow capacity represented by the slack variable value greater than 0.0000. Thus, if the slack variable of node 2 is greater than 0.0000, any changes of arrival rates of node 2,  $\lambda_{S \rightarrow 2}$  within  $a \leq \Delta_2 \leq b$  or  $\lambda_{S \rightarrow 2} \in [\alpha - a, \alpha + b]$  has no effect on the current optimal solution and the value of its objective function. Note that  $\alpha$  is the optimal flow in node 2 while  $a$  and  $b$  are the lower and upper bounds of the optimal flow generated by the network flow model. The dual price greater than 0.0000 meanwhile indicates that its inflow capacity has fully been utilised represented by its slack variable value of 0.0000. Thus, any increment or decrement in its arrival rate will increase or decrease to  $Z + \Delta_2$ , where  $Z$  is the current value of the objective function. This dual price stays valid for a particular lower and upper bound of the optimal arrival rate generated by the model,  $\lambda_{S \rightarrow 2} \in [\alpha - a, \alpha + b]$ ; i.e. before the current solution mix changes.

The second case is the new optimal arrival rate is out of an allowable range. For example, the new optimal arrival rate to node 2, i.e.  $\lambda_{S \rightarrow 2} \notin [\alpha - a, \alpha + b]$ .

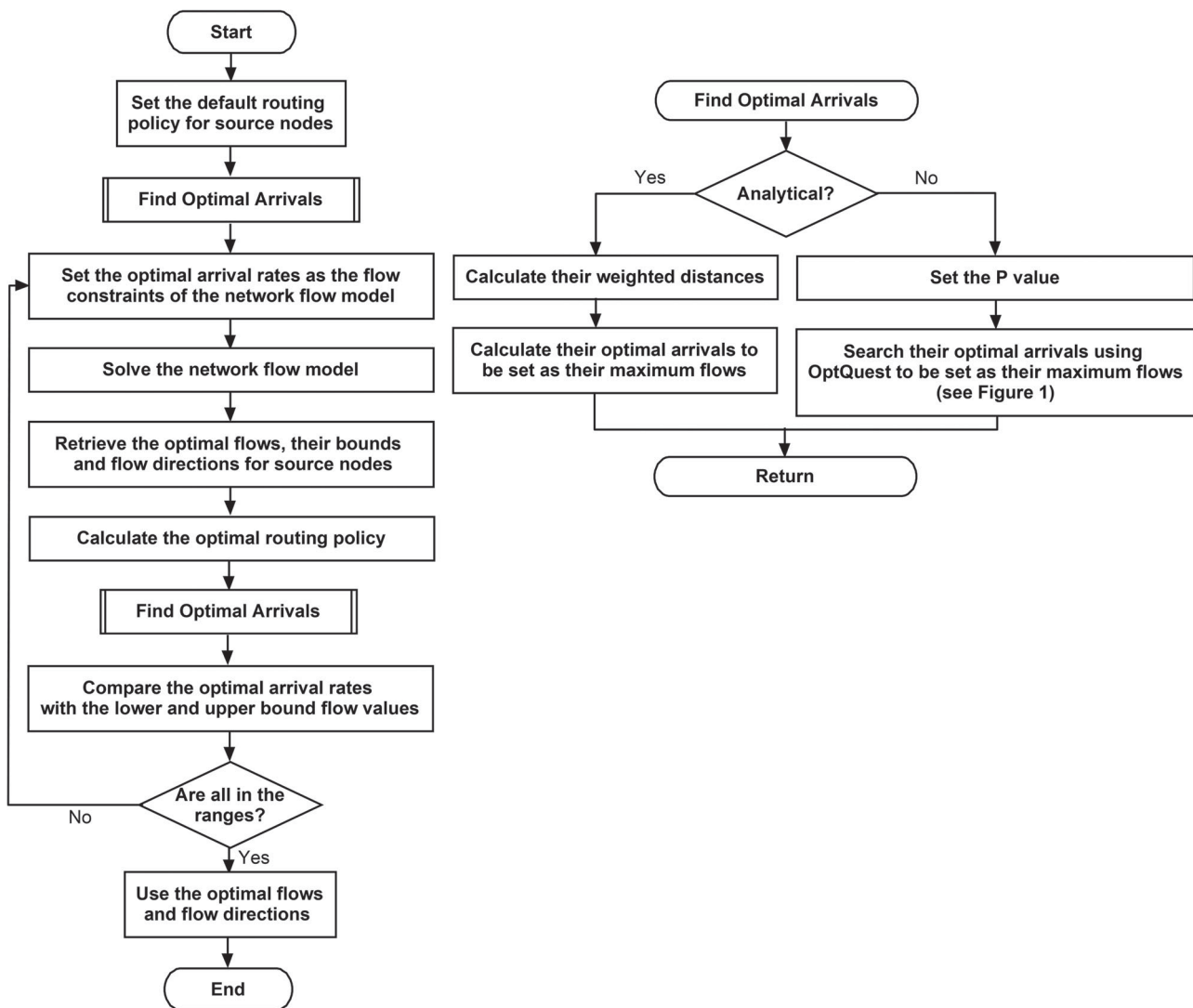


**Figure 4.** Finding the optimal arrival rates of source nodes.

In this case, we have to re-solve the model by changing the optimal arrival rate to node 2 to  $\lambda_{S \rightarrow 2}$  while keeping the same arrival rates to other source nodes. This step is repeated until all arrival rate values of source nodes are within their allowable ranges. The processes of finding the optimal arrival rates to source nodes are illustrated in Figure 4.

### 3.6. Analysing the impact of the optimal flow to the performance of the topological network

The optimal arrival rates to source nodes are then input to real distance analytical and simulation models to analyse their impacts on the network's performance. The main purpose of the simulation model is to validate the analytical model. The real distance simulation model uses the exact distance of each arrival source in

a source node to its downstream nodes and accepts its routing probabilities. The simulation model is an extended version of the *M/G/C/C* simulation model discussed in R. Khalid et al. (2013).

In brief, each arrival source is modelled using a *Create* module which generates pedestrians according to a specified arrival rate. The pedestrians then travel to the end of source nodes and downstream nodes based on routing probabilities specified using a *Decide* module. If the nodes are full, the pedestrians are temporarily queued in a *Seize* module and will only travel when there are available spaces based on the capacity of the nodes. Their movement through the nodes is simulated using a *Hold* module. Its number in queue denotes the current number of residing pedestrians in the nodes while the waiting time spent by the pedestrians in the queue denotes their travel times. Other

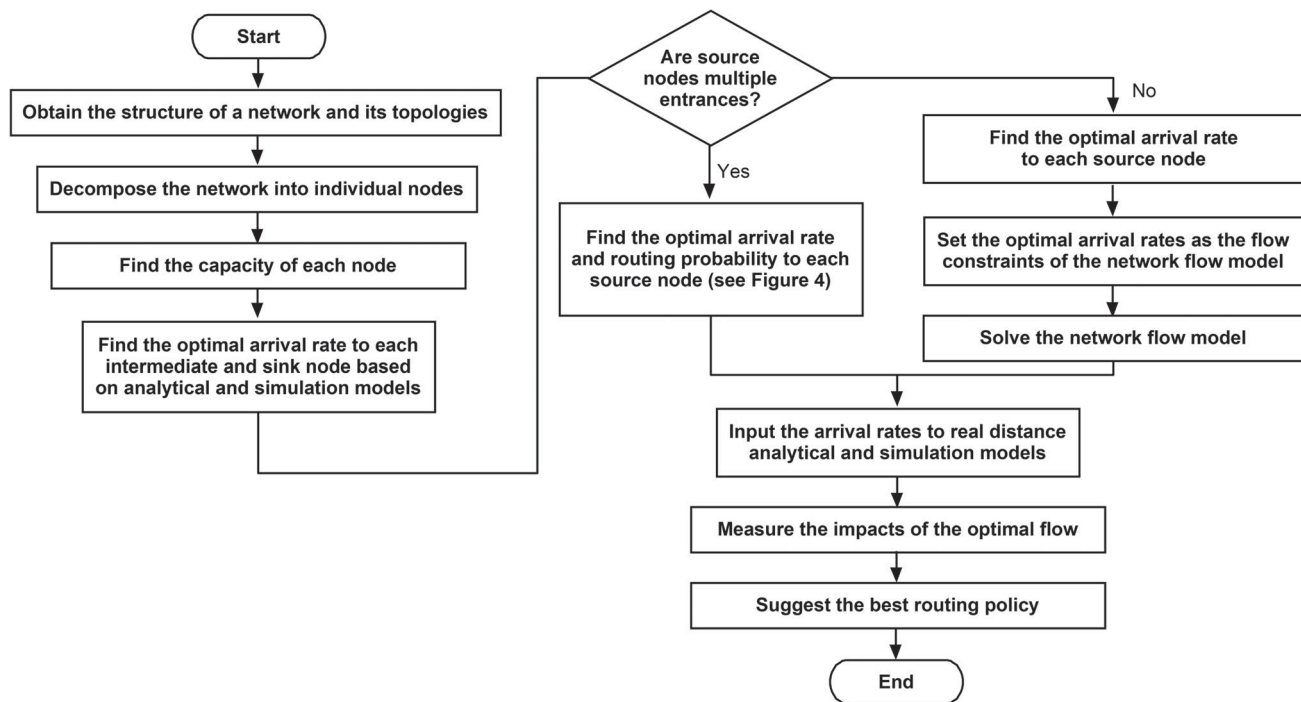


**Figure 5.** Steps to calculate the optimal routing policy.

modules (e.g. *Signal* and *Remove*) are used to temporarily remove the pedestrians to update their current attribute values or permanently remove them to flow to downstream nodes.

All the parameters of the simulation model; e.g. arrival rates, lengths and widths of the nodes, current travel speed and routing probabilities are stored in variables. All attribute values; e.g. the travel distance and current location which is unique for each pedestrian are stored in attributes and attached to the pedestrians. The variables and attributes are declared and assigned values using an *Assign* module which can directly be accessed via a *Variable* spreadsheet. Various setup option parameters before running the model; e.g. the number of replications and replication length are set in the *Run Setup* dialog box. However, some of the model parameters; e.g. arrival rates and routing probabilities can easily be made accessible to users by uploading the model to Process Analyzer which eases them to interactively analyse the performance of a network based on various parameter changes and scenarios.

Both models should replicate all topologies and the dynamic flow from node to node. For any topologies, the arrival rate to a particular node is the total proportional outflow of all its connected upstream nodes. The arrival rate determines the flow through the node and

its throughput. The proportion of the throughput will then be the arrival rate to its other downstream nodes. The processes continue for all other topologies. The throughput of the whole network generated by both models are then compared and justified. Figure 5 summarises the steps taken to calculate the best routing policy.

#### 4. Tuanku Syed Putra hall (DTSP) as a case study

Our modelling of pedestrian flow in the DTSP (Kawsar et al., 2013) was performed as follows. We first obtained its structure and retrieved all available corridors and their topologies as in Figure 6. All corridors are numbered consecutively. Corridors 6, 7, 8, 9, 10 and 11 are source corridors, corridor 3a is an intermediate corridor while corridors 1, 2, 3b, 3c, 12, 13, 14 and 15 are exit corridors. The detailed information in terms of their lengths and widths (in metre), available entrances (the number and distance to the end of the source corridors) is shown in Table 1. Each entrance represents the entrance point of a row of seats.

The seats are clustered using alphabets *S*, *T*, *U*, *V*, *W*, *X*, *Y* and *Z* whose numbers are 220, 220, 309, 259, 100, 55, 98 and 77 seats respectively. *S* and *T* are the sources for corridor 11, each of which has 8 entrances. *U* and *V* are the sources for corridor 10, each of which has 5

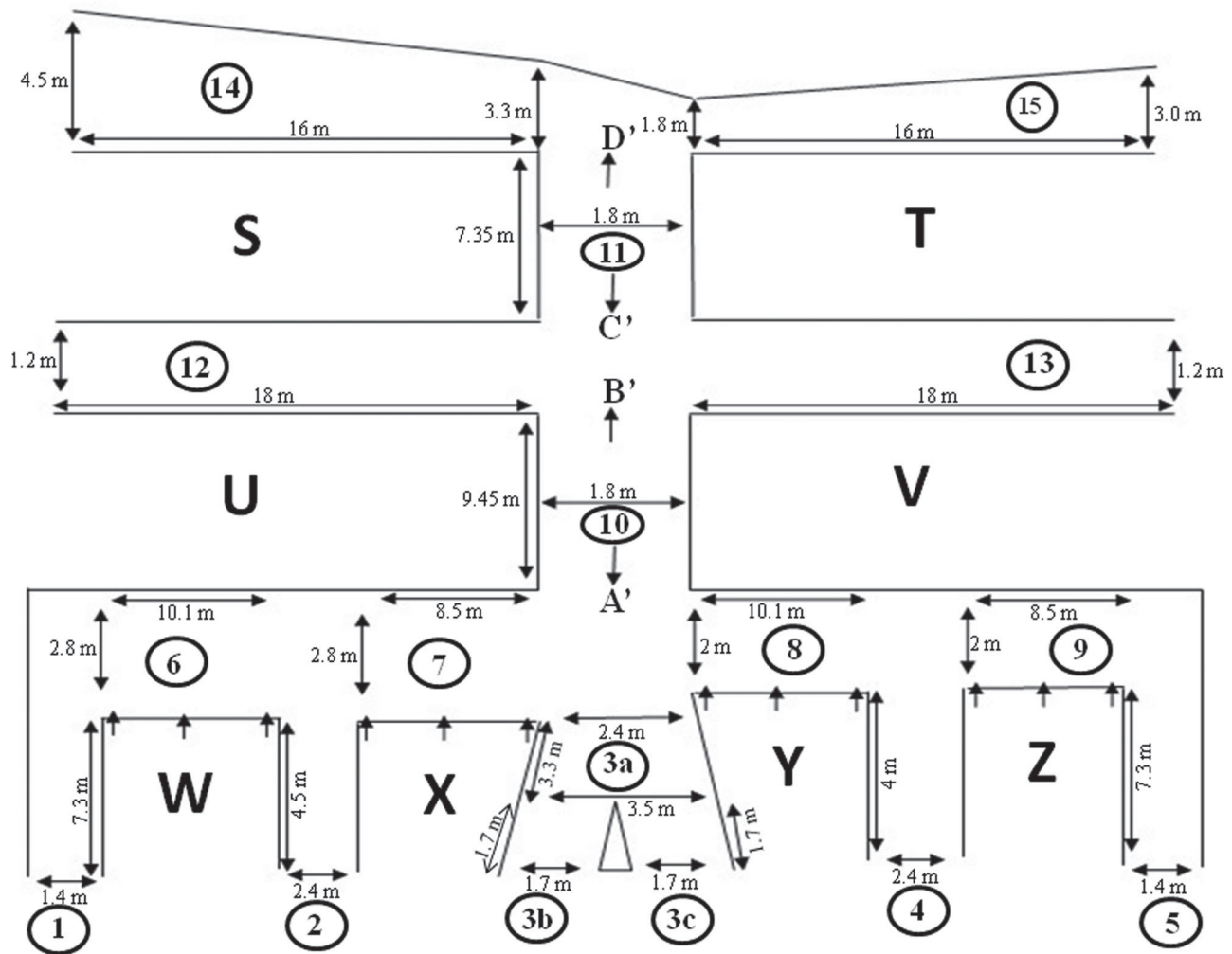


**Figure 6.** DTSP's structures and its available corridors (Kawsar et al., 2013).

entrances. W, X, Y and Z are the sources for corridors 6, 7, 8 and 9, each of which has 3 entrances respectively. Initially, all pedestrians are assumed in their seats and no pedestrians are in any corridors.

Our next step was to construct an analytical *M/G/C/C* program and verify its accuracy by comparing its results with analytical results reported in previous studies; e.g. Cruz and Smith (2007), Cruz et al. (2005) and Mitchell and Smith (2001). To validate the analytical results, we first developed an *M/G/C/C* weighted distance simulation model using Arena. Its outputs were compared with the outputs of the available *M/G/C/C* simulation model; i.e. *MGCCSimul* (Cruz et al., 2005; Mitchell & Smith, 2001). Both simulation models generated almost similar performance outputs for various input parameters of arrival rates, lengths and widths as reported in Cruz et al. (2005).

Comparing our analytical and simulation models' outputs, we found that there was a small range

of arrival rates of each corridor where both models showed significant discrepancies. The range always took place at the arrival rates starting the blocking. The findings were reported in R. Khalid et al. (2013) and Cruz et al. (2005). Based on the weighted simulation model, we then constructed the real distance simulation model of a source network with multiple entrances. The models were used to search the optimal arrival rate of each corridor maximising its throughput using OptQuest. Its optimal arrival rate based on the analytical model was also derived.

The optimal arrival rates to available corridors in the DTSP generated by both models were then input into the network flow models. Solving the network flow models and manipulating relevant flow constraints based on relevant routing policies gave us various sets of the optimal arrival rates maximising the DTSP's overall throughput. The optimal arrival rates were then input into real analytical (*real\_analytic*) and

**Table 1.** Detail information on source corridors.

Source Corridor	No. of Entrance	Length × Width (metre)	Distance of Entrance (metre)	Weighted Length (metre)	Relevant Exit/Intermediate Corridor
6	3	10.1 × 2.8	$L_1 = 0.73125, L_2 = 5.00625, L_3 = 0.73125$	2.156	1 and 2
7	3	8.5 × 2.8	$L_1 = 0.73125, L_2 = 3.88125, L_3 = 0.73125$	1.780	2 and 3
8	3	10.1 × 2.0	$L_1 = 0.73125, L_2 = 5.00625, L_3 = 0.73125$	2.156	3 and 4
9	3	8.5 × 2.0	$L_1 = 0.73125, L_2 = 3.88125, L_3 = 0.73125$	1.780	4 and 5
10	20	9.45 × 1.8	$L_1 = L_2 = L_3 = L_4 = 0.9;$ $L_5 = L_6 = L_7 = L_8 = 1.8;$ $L_9 = L_{10} = L_{11} = L_{12} = 2.7;$ $L_{13} = L_{14} = L_{15} = L_{16} = 3.6;$ $L_{17} = L_{18} = L_{19} = L_{20} = 4.5$	2.700	3, 12, and 13
11	16	7.35 × 1.8	$L_1 = L_2 = L_3 = L_4 = 0.91;$ $L_5 = L_6 = L_7 = L_8 = 1.82;$ $L_9 = L_{10} = L_{11} = L_{12} = 2.73;$ $L_{13} = L_{14} = L_{15} = L_{16} = 3.64$	2.275	12, 13, 14 and 15

real distance simulation (*real\_sim*) models to measure their impacts on the performances of all corridors.

#### 4.1. Two practical routing policies

We consider two practical routing policies to flow pedestrians out of the DTSP. For each policy, we find the optimal arrival rates to source corridors and measure their impacts on the performance of all available corridors using real distance analytical and simulation models. Their performances are then compared to justify the best policy for flowing pedestrians. The routing policies are:

##### (a) Routing pedestrians to their nearest exit corridors

Pedestrians from source corridors 6, 7, 8, 9, 10 and 11 travel to their nearest exit corridors. They are thus split into half to travel to one side of the corridor. For example, pedestrians from seating *W* first enter corridor 6. 50% of them travel to corridor 1 while the others travel to corridor 2. The same logic applies to corridor 10. Pedestrians from seating *U* and *V* first enter corridor 10. 50% of them travel to exit corridors 12 and 13 while the others travel to corridor 3a to join pedestrians from corridors 7 and 8. All of them finally exit the DTSP through exit corridors 3b or 3c.

##### (b) Routing pedestrians maximising the overall throughput

This policy finds the optimal arrival rate of pedestrians to each source corridor and routing probability

to relevant downstream corridors maximising the throughput of the DTSP. In this strategy, some percentages of pedestrians enter the source corridors with relevant arrival rates and travel to either one side of the corridors to join pedestrians in the downstream corridors.

#### 4.2. Casting the DTSP's policies as a network flow model

The flow of pedestrians in the DTSP can be casted as a network flow diagram as in Figure 7. The nodes symbolise the corridors while the arrows represent pedestrians' movement from their seats to the downstream corridors. The objective is to find the optimal arrival rates to source corridors 6, 7, 8, 9, 10 and 11 ( $x_{T \rightarrow S} = x_{S \rightarrow 6} + x_{S \rightarrow 7} + x_{S \rightarrow 8} + x_{S \rightarrow 9} + x_{S \rightarrow 10} + x_{S \rightarrow 11}$ ) maximising the throughput of the hall; i.e. the total throughputs of all exit corridors 1, 2, 3b, 3c, 4, 5, 12, 13, 14 and 15 ( $x_{1 \rightarrow T} + x_{2 \rightarrow T} + x_{3b \rightarrow T} + x_{3c \rightarrow T} + x_{4 \rightarrow T} + x_{5 \rightarrow T} + x_{12 \rightarrow T} + x_{13 \rightarrow T} + x_{14 \rightarrow T} + x_{15 \rightarrow T} = x_{T \rightarrow S}$ ). To find the optimal arrival rates, the optimal arrival rate to each individual source, intermediate and exit corridor maximising its throughput has to be retrieved. The optimal arrival rate for each corridor and its performance based on analytical (denoted as *analytic*) and simulation (*sim*) models are shown in Table 2.  $\lambda$ ,  $\theta$  and  $p(c)$  respectively represent the arrival rate, throughput and blocking probability of the corridor. Any values bigger than the optimal arrival rate decrease the throughput and increase the blocking.

Note that the initial optimal arrival rates to the source corridors are calculated based on the distance

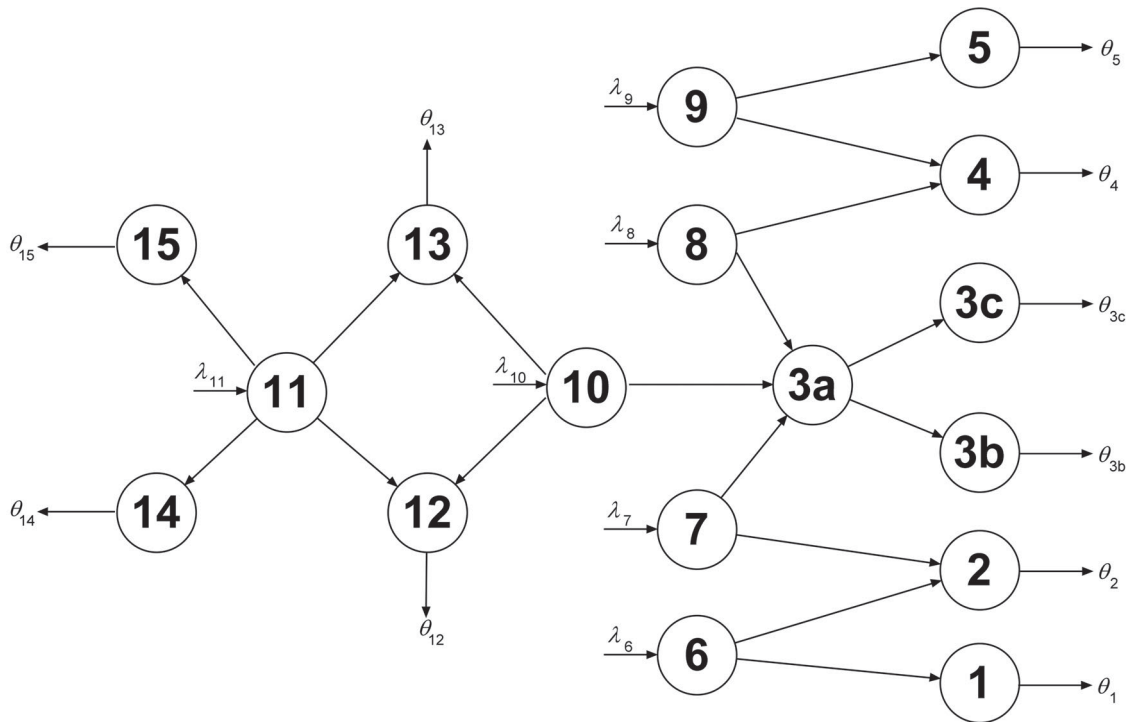


**Figure 7.** DTSP's network flow diagram.

**Table 2.** Arrival rates maximising corridor throughputs.

Corridor	Model	$\lambda$	$\theta$	$p(c)$	Corridor	Model	$\lambda$	$\theta$	$p(c)$
6	analytic	14.1800	14.0436	0.0096	3b	analytic	1.8800	1.6452	0.1249
	sim	14.0992	14.0877	0.0000		sim	1.5150	1.4021	0.0740
7	analytic	14.4600	14.2904	0.0117	3c	analytic	1.8800	1.6452	0.1249
	sim	14.0094	14.0198	0.0000		sim	1.5150	1.4021	0.0740
8	analytic	10.1100	9.9744	0.0134	4	analytic	2.5800	2.4973	0.0321
	sim	9.7610	9.7558	0.0000		sim	2.3000	2.2094	0.0382
9	analytic	10.2900	10.1213	0.0164	5	analytic	1.4900	1.4478	0.0283
	sim	9.4688	9.4747	0.0000		sim	1.3473	1.3182	0.0187
10	analytic	6.7500	6.6422	0.0160	12	analytic	1.3000	1.2792	0.0160
	sim	6.3838	6.3476	0.0044		sim	1.2617	1.2596	0.0000
11	analytic	6.2100	6.0807	0.0208	13	analytic	1.3000	1.2792	0.0160
	sim	5.7595	5.6940	0.0120		sim	1.2617	1.2596	0.0000
3a	analytic	3.1600	3.0614	0.0312	14	analytic	4.2500	4.2343	0.0037
	sim	2.7000	2.6596	0.0152		sim	4.5000	4.4912	0.0000
1	analytic	1.4900	1.4478	0.0283	15	analytic	2.6100	2.5886	0.0082
	sim	1.3473	1.3182	0.0187		sim	2.7029	2.6989	0.0000
2	analytic	2.5800	2.5077	0.0280					
	sim	2.3081	2.5927	0.0218					

where pedestrians are assumed to travel to their nearest downstream corridors located at the both ends of the corridors; i.e.  $P_6 = P_7 = P_8 = P_9 = P_{10} = P_{11} = 0.5$  as considered in the first routing policy. In this case, the weighted distance for corridor 6 with 3 arrival sources based on analytical is thus  $L'_6 = \frac{L_{6,1 \rightarrow 1} + 0.5L_{6,2 \rightarrow 1} + 0.5L_{6,2 \rightarrow 2} + L_{6,3 \rightarrow 2}}{3} = [0.73125 + 0.5(5.00625) + 0.5(5.00625) + 0.73125]/3 = 2.1560$  m while the weighted distance for corridor 11 with 16 arrival sources is  $2[2(0.91) + 2(1.82) + 2(2.73) + 2(3.64)]/16 = 2.2750$  m (see Table 1). The optimal

arrival rates for simulation are generated using OptQuest based on 30 potential scenarios bounded by relevant ranges, each of which is run for 20,000 s and 10 replications. In average, OptQuest takes 1500 min to report the optimal arrival for each corridor.

All the corridors' optimal arrival rates generated by each model are then separately set as their inflow capacities in the network flow model to find the optimal arrival rates to the source corridors. Thus, each policy has two sets of optimal arrival rates. The first



set is based on analytical while the second set is based on simulation.

### 4.3. Modelling the routing policies

For the first routing policy, we must ensure that the outflow of each source corridor is equal to its inflow; i.e.  $x_{S \rightarrow 6} = x_{6 \rightarrow 1} + x_{6 \rightarrow 2}$ ,  $x_{S \rightarrow 7} = x_{7 \rightarrow 2} + x_{7 \rightarrow 3a}$ ,  $x_{S \rightarrow 8} = x_{8 \rightarrow 3a} + x_{8 \rightarrow 4}$ ,  $x_{S \rightarrow 9} = x_{9 \rightarrow 4} + x_{9 \rightarrow 5}$ ,  $x_{S \rightarrow 10} = x_{10 \rightarrow 3a} + x_{10 \rightarrow 12} + x_{10 \rightarrow 13}$  and  $x_{S \rightarrow 11} = x_{11 \rightarrow 12} + x_{11 \rightarrow 13} + x_{11 \rightarrow 14} + x_{11 \rightarrow 15}$  (see Figure 7). Additionally, the inflow to each corridor must be smaller or equal to its optimal arrival rate to avoid any blockages (see Table 2). For example, the inflow to source corridor 6 for the analytical model must not exceed 14.1800; i.e.  $x_{S \rightarrow 6} \leq 14.1800$ . The same concept is also applied for intermediate and exit corridors. For example, the flow conservation for intermediate corridor 3a is  $x_{7 \rightarrow 3a} + x_{8 \rightarrow 3a} + x_{10 \rightarrow 3a} \leq 3.1600$  while that for exit corridor 12 is  $x_{10 \rightarrow 12} + x_{11 \rightarrow 12} \leq 1.3000$ . We must also ensure that pedestrians are split into half with the travel probability of 0.5 and directed to travel to their nearest corridors. Thus, we must set the outflow constraints of each corridor; i.e.  $x_{6 \rightarrow 1} = x_{6 \rightarrow 2}$ ,  $x_{7 \rightarrow 2} = x_{7 \rightarrow 3a}$ ,  $x_{8 \rightarrow 3a} = x_{8 \rightarrow 4}$ ,  $x_{9 \rightarrow 4} = x_{9 \rightarrow 5}$ ,  $x_{10 \rightarrow 3a} = x_{10 \rightarrow 12} + x_{10 \rightarrow 13}$ ,  $x_{11 \rightarrow 12} + x_{11 \rightarrow 13} = x_{11 \rightarrow 14} + x_{11 \rightarrow 15}$ .

For the second routing policy, we have to remove the outflow constraints imposed in the first routing policy. This removal allows the network flow model to flexibly search the optimal flow in each source corridor. Based on the optimal flow, we can calculate the pedestrian routing probability to the ends of the source corridor. For the analytical model, this optimal value depends on the corridor's weighted travel distance which cannot be calculated if its optimal routing probability is unknown. As discussed in Section 3.6, we initially solved the network flow model using the corridors' optimal arrival rates as in the first policy without imposing the outflow constraints; i.e. by removing the constraint  $x_{6 \rightarrow 1} = x_{6 \rightarrow 2}$ ,  $x_{7 \rightarrow 2} = x_{7 \rightarrow 3a}$ ,  $x_{8 \rightarrow 3a} = x_{8 \rightarrow 4}$ ,  $x_{9 \rightarrow 4} = x_{9 \rightarrow 5}$ ,  $x_{10 \rightarrow 3a} = x_{10 \rightarrow 12} + x_{10 \rightarrow 13}$  and  $x_{11 \rightarrow 12} + x_{11 \rightarrow 13} = x_{11 \rightarrow 14} + x_{11 \rightarrow 15}$ . Solving the model gives us a new initial set of the optimal flow in the source corridors. Using the optimal flow, we can calculate the routing probability for each source corridor. Based on the routing probability and its flow direction, we calculate the corridor's new weighted travel distance

which is then used to find the corridor's new optimal arrival rate for both the analytical and simulation models. The new optimal arrival rate is then compared to the lower and upper bound of the optimal flow. All network flow models are solved using Lingo software (<http://www.lindo.com>). In average, Lingo takes 0.05 s to solve each network flow model.

### 4.4. Measuring the impacts of the optimal arrival rates on the DTSP's performance

The optimal arrival rate to each source corridor is input to analytical (*real\_analytic*) and simulation (*real\_sim*) models of the DTSP to evaluate the flow performance of the two routing policies. The routing policies in *real\_sim* can flexibly be handled by changing the values of probability variables of the source corridors during the analysis. For the first routing policy, all probabilities of source corridors have to be set to 0.5; i.e.  $P_6 = P_7 = P_8 = P_9 = P_{10} = P_{11} = 0.5$ . For the second routing policy, the optimal routing probability of each source has to be calculated based on the flow value generated by the network flow model.

## 5. Results and analysis

For each routing policy, the optimal arrival rates to the source corridors generated by the network flow model based on the analytical model are first analysed using *real\_analytic*. Its performance is validated using *real\_sim*. We next analyse the optimal arrival rates generated by the network flow model based on the simulation model. Its performance is first analysed using *real\_sim* and then confirmed using *real\_analytic*. All simulation results are based on 30 replications with the confidence interval is 95% ( $\alpha = 0.05$ ). Each replication is run for 20,000 s and analysed using Process Analyzer. In average, Process Analyzer takes 330 min to validate each of the policies.

### 5.1. Performances of the first routing policy

Using the optimal arrival rates of the analytical model in Table 2, the network flow model for the first policy reports that the flow values of  $x_{S \rightarrow 6} = 2.9800$ ,  $x_{S \rightarrow 7} = 2.1800$ ,  $x_{S \rightarrow 8} = 2.1800$ ,  $x_{S \rightarrow 9} = 2.9800$ ,  $x_{S \rightarrow 10} = 1.9600$  and  $x_{S \rightarrow 11} = 3.2400$  generate the maximum total flow of 15.5200. Inputting the flow values into *real\_analytic* generates the overall throughput

of 15.0831. The detailed performance of the first routing policy is shown in Table 3. The maximum blocking probability is observed in corridor 4 with the value of 0.0321 (3.21%). The small blockings in all corridors confirm smooth flow in all routes.

To validate the performance, we feed the flow values to *real\_sim*. The model however generates the overall throughput of 12.7776. The inconsistency of the throughputs is much influenced by intermediate corridor 3a. The optimal arrival rate for corridor 3a based on the simulation model is only 2.7000 (compared to 3.1600 based on the analytical model); see Table 2. In *real\_sim*, the arrival rate of 3.1622 generated from half of the throughputs of corridors 7, 8 and 10 causes a massive blocking in corridor 3a decreasing its throughput. This small throughput then causes the small arrival rate to exit corridors 3a and 3b (in spite of the fact that they can support the arrival rate of 1.5150) which eventually decreases the throughputs of the two exit corridors. For other exit corridors, both models report almost the same arrival rates from their source corridors. However, since the optimal arrival rates supported by the simulation model are slightly smaller than the analytical model in most of our analyses, the overall throughput generated by *real\_sim* is much smaller than *real\_analytic*.

We then restrict the same flow to source corridors 6, 7, 8 and 9 (i.e.  $x_{S \rightarrow 6} = x_{S \rightarrow 7} = x_{S \rightarrow 8} = x_{S \rightarrow 9}$ ) and let the network flow model to flexibly adjust the flow to corridors 10 and 11. Under this restriction, Lingo reports that  $x_{S \rightarrow 6} = x_{S \rightarrow 7} = x_{S \rightarrow 8} = x_{S \rightarrow 9} = 2.5800$ ,  $x_{S \rightarrow 10} = 1.1600$  and  $x_{S \rightarrow 11} = 4.0400$  also generate the maximum total flow of 15.5200. Feeding the flow values into *real\_analytic* generates the overall throughput of 15.1672; i.e. an increase of 0.0841 from the flexible rate strategies. The throughputs of all corridors are as in Table 3. There are decreases in the throughputs of corridors 1 and 2; i.e. 0.1579 each. The decreases are however balanced with the increases in the throughputs of corridors 14 and 15 which increase as much as 0.2000 each; and this contributes to a slight increase in the throughput of the DTSP. Feeding the flow values into *real\_sim* also generates a better overall throughput; i.e. 13.3806.

We then search the optimal arrival rates of source corridors based on the simulation model by inputting the optimal arrival rate of each source corridor to the network flow model. The model reports that the flow values of  $x_{S \rightarrow 6} = 2.6946$ ,  $x_{S \rightarrow 7} = 1.9216$ ,

$x_{S \rightarrow 8} = 1.9054$ ,  $x_{S \rightarrow 9} = 2.6946$ ,  $x_{S \rightarrow 10} = 1.5730$  and  $x_{S \rightarrow 11} = 3.4738$  will optimise the flow of 14.2630. Inputting the flow values into *real\_sim* generates the overall throughput of 14.1233 while *real\_analytic* generates the overall throughput of 14.2439. The throughputs of all corridors are as in Table 4. There is a small discrepancy between the two throughputs since *real\_analytic* uses the values without causing any blockings in all corridors.

Restricting the same flow to source corridors 6, 7, 8 and 9 (i.e.  $x_{S \rightarrow 6} = x_{S \rightarrow 7} = x_{S \rightarrow 8} = x_{S \rightarrow 9}$ ) yields  $x_{S \rightarrow 6} = x_{S \rightarrow 7} = x_{S \rightarrow 8} = x_{S \rightarrow 9} = 2.300$ ,  $x_{S \rightarrow 10} = 0.8000$ ,  $x_{S \rightarrow 11} = 4.2468$  with the same maximum total flow of 14.2468. Using these flow values, *real\_sim* and *real\_analytic* generate the throughput of 14.1009 and 14.2293 respectively. Both models report that there are small blockings along all routes. Simulation and analytical results show that the flexible arrival rates produce a better throughput.

## 5.2. Performances of the second routing policy

For the second routing policy, the weighted travel distance of each source corridor depends on the routing probability of pedestrians from the corridor to their downstream corridors. Since the optimal routing probability value is unknown, their weighted travel distance cannot be calculated. As mentioned, our strategy is to first use the weighted travel distance of each source corridor as in the first routing policy (see Table 2) and let Lingo freely find the optimal rate of the corridor.

Using the weighted travel distances, Lingo reported  $x_{S \rightarrow 6} = 1.4900$ ,  $x_{S \rightarrow 7} = 5.7400$ ,  $x_{S \rightarrow 8} = 2.5800$ ,  $x_{S \rightarrow 9} = 1.4900$ ,  $x_{S \rightarrow 10} = 2.6000$  and  $x_{S \rightarrow 11} = 6.2100$  generate the maximum flow of 20.1100 with the conditions that  $x_{6 \rightarrow 1} = 1.4900$ ,  $x_{6 \rightarrow 2} = 0.0000$ ,  $x_{7 \rightarrow 2} = 2.5800$ ,  $x_{7 \rightarrow 3a} = 3.1600$ ,  $x_{8 \rightarrow 3a} = 0.0000$ ,  $x_{8 \rightarrow 4} = 2.5800$ ,  $x_{9 \rightarrow 4} = 0.0000$ ,  $x_{9 \rightarrow 5} = 1.4900$ ,  $x_{10 \rightarrow 3a} = 0.0000$ ,  $x_{10 \rightarrow 12} = 1.3000$  and  $x_{10 \rightarrow 13} = 1.3000$ ,  $x_{11 \rightarrow 12} = 0.0000$ ,  $x_{11 \rightarrow 13} = 0.0000$ ,  $x_{11 \rightarrow 14} = 4.2500$  and  $x_{11 \rightarrow 15} = 1.9600$ . Based on the optimal flow, we then calculate the routing probability of each source corridor to its downstream corridors. For example, consider corridor 6. The network flow model reports that  $x_{S \rightarrow 6} = 1.4900$  maximises the flow with the conditions that  $x_{6 \rightarrow 1} = 1.4900$  and  $x_{6 \rightarrow 2} = 0.0000$ ; i.e.  $P_6 = 1$ . Thus, all pedestrians in corridor 6 should only travel to corridor 1

**Table 3.** Analytical results for the first routing policy.

Corridor Type	Corridor	Model	Flexible Arrival Rate			Same Arrival Rate for Corridor 6, 7, 8 and 9		
			$\lambda$	$\theta$	$p(c)$	$\lambda$	$\theta$	$p(c)$
Source	6	<i>real_analytic</i>	2.9800	2.9800	0.0000	2.5800	2.5800	0.0000
		<i>real_sim</i>		2.9775	0.0000		2.5808	0.0000
	7	<i>real_analytic</i>	2.1800	2.1800	0.0000	2.5800	2.5800	0.0000
		<i>real_sim</i>		2.1790	0.0000		2.5800	0.0000
	8	<i>real_analytic</i>	2.1800	2.1800	0.0000	2.5800	2.5800	0.0000
		<i>real_sim</i>		2.1819	0.0000		2.5796	0.0000
	9	<i>real_analytic</i>	2.9800	2.9800	0.0000	2.5800	2.5800	0.0000
		<i>real_sim</i>		2.9771	0.0000		2.5790	0.0000
	10	<i>real_analytic</i>	1.9600	1.9600	0.0000	1.1600	1.1600	0.0000
		<i>real_sim</i>		1.9635	0.0000		1.1617	0.0000
	11	<i>real_analytic</i>	3.2400	3.2400	0.0000	4.0400	4.0400	0.0000
		<i>real_sim</i>		3.2427	0.0000		4.0412	0.0000
Intermediate	3a	<i>real_analytic</i>	3.1600	3.0614	0.0312	3.1600	3.0614	0.0312
		<i>real_sim</i>		3.1622	0.2647		2.3101	0.2676
Exit	1	<i>real_analytic</i>	1.4900	1.4478	0.0283	1.2900	1.2899	0.0001
		<i>real_sim</i>		1.4888	0.1903		1.2904	0.0000
	2	<i>real_analytic</i>	2.5800	2.5077	0.0280	2.5800	2.5077	0.0280
		<i>real_sim</i>		2.5783	0.2387		2.5804	0.2377
	3b	<i>real_analytic</i>	1.5307	1.5020	0.0187	1.5307	1.5020	0.0187
		<i>real_sim</i>		1.1611	0.0000		1.1551	0.0000
	3c	<i>real_analytic</i>	1.5307	1.5020	0.0187	1.5307	1.5020	0.0187
		<i>real_sim</i>		1.1611	0.0000		1.1551	0.0000
	4	<i>real_analytic</i>	2.5800	2.4973	0.0321	2.5800	2.4973	0.0321
		<i>real_sim</i>		2.5795	0.2551		2.5793	0.2597
	5	<i>real_analytic</i>	1.4900	1.4478	0.0283	1.2900	1.2899	0.0001
		<i>real_sim</i>		1.4886	0.2244		1.2895	0.0000
	12	<i>real_analytic</i>	1.3000	1.2792	0.0160	1.3000	1.2792	0.0160
		<i>real_sim</i>		1.3016	0.0000		1.3007	0.0000
	13	<i>real_analytic</i>	1.3000	1.2792	0.0160	1.3000	1.2792	0.0160
<i>real_sim</i>			1.3016	0.0000		1.3007	0.0000	
14	<i>real_analytic</i>	0.8100	0.8100	0.0000	1.0100	1.0100	0.0000	
	<i>real_sim</i>		0.8107	0.0000		1.0103	0.0000	
15	<i>real_analytic</i>	0.8100	0.8100	0.0000	1.0100	1.0100	0.0000	
	<i>real_sim</i>		0.8111	0.0000		1.0103	0.0000	
Throughput			$\theta_{Analytic} = 15.0831, \theta_{Sim} = 12.7776$			$\theta_{Analytic} = 15.1672, \theta_{Sim} = 13.3806$		

to exit. The weighted distance for this flow is  $[1(0.73125) + 1(5.00625) + 1(10.1 - 0.73125)]/3 = 5.0354$  m. In this case, 10.1 is the length of corridor 6 (see Table 1). For corridor 7,  $x_{S \rightarrow 7} = 5.7400$  with  $x_{7 \rightarrow 2} = 2.5800$  and  $x_{7 \rightarrow 3a} = 3.1600$ ; i.e.  $P_7 = 2.5800/5.7400 = 0.4495$  maximises the flow in the network. This reflects that 44.95% of pedestrians in corridor 7 should travel to corridor 2 while the others travel to corridor 3a to exit. The weighted travel distance based on the flow is  $[1(0.73125) + 0.4495(3.88125) + 0.5505(3.88125) + 1(0.73125)]/3 = 1.7813$  m. The same calculation is also applied to corridor 10. Since  $P_{10} = 0$ ; i.e. all pedestrians in corridor 10 should only travel to corridors 12 and 13 to exit. Its weighted distance is thus  $2[0.9 + 1.8 + 2.7 + 3.6 + 4.5 + (9.45 - 4.5) + (9.45 - 3.6) + (9.45 - 2.7) + (9.45 - 1.8) + (9.45 - 0.9)]/20 = 4.950$  m. Using the weighted distance, the new optimal arrival rate is then derived. Table 5 shows the routing probability, the new weighted travel distance and the new optimal arrival rate for each source corridor based on the analytical model. Table 6 meanwhile shows the

sensitivity analysis results reported by Lingo for the second routing policy.

From Table 6, the dual price of each source corridor except corridor 11 is 0.0000. This indicates that any changes of arrival rates to the corridor within its allowable range will not change the current solution and the value of the hall throughput since there is still an unused inflow capacity represented by its slack variable value. For example, any changes of arrival rates to corridor 10 within  $4.1500 \leq \Delta_{10} < \infty$  or  $\lambda_{10} \in [2.600, \infty)$  has no effect on the current solution and throughput value. The dual price of corridor 11 is 1.0000 since its inflow capacity has fully been utilised represented by its slack variable value of 0.0000. Thus, any decreases or increases in its arrival rate will decrease or increase the objective function value to  $20.1100 + \Delta_{11}$ . This dual price stays valid for  $\lambda_{11} \in [4.2500, 6.8600]$ ; i.e. before the current solution mix changes.

The next step is to calculate the new optimal arrival rate of each source corridor based on its new weighted travel distance which in turn depends on the optimal

**Table 4.** Simulation results for the first routing policy.

Corridor Type	Corridor	Flexible Arrival Rate			Same Arrival Rate for Corridor 6, 7, 8 and 9			
		$\lambda$	$\theta$	$p(c)$	$\lambda$	$\theta$	$p(c)$	
Source	6	2.6946	2.6980	0.0000	2.3000	2.3002	0.0000	
	7	1.9216	1.9238	0.0000	2.3000	2.3005	0.0000	
	8	1.9054	1.9055	0.0000	2.3000	2.3025	0.0000	
	9	2.6946	2.6925	0.0000	2.3000	2.3009	0.0000	
	10	1.5730	1.5741	0.0000	0.8000	0.8007	0.0000	
	11	3.4738	3.4787	0.0000	4.2468	4.2484	0.0000	
Intermediate	3a	2.7017	2.6961	0.0017	2.7019	2.6746	0.0104	
Exit	1	1.3490	1.3106	0.0277	1.1501	1.1502	0.0000	
	2	2.3109	2.2885	0.0098	2.3004	2.2697	0.0120	
	3b	1.3481	1.3480	0.0000	1.3373	1.3372	0.0000	
	3c	1.3481	1.3479	0.0000	1.3373	1.3372	0.0000	
	4	2.2990	2.2287	0.0306	2.3017	2.2109	0.0389	
	5	1.3463	1.3382	0.0048	1.1505	1.1507	0.0000	
	12	1.2632	1.2611	0.0000	1.2623	1.2615	0.0000	
	13	1.2632	1.2611	0.0000	1.2623	1.2615	0.0000	
	14	0.8697	0.8696	0.0000	1.0621	1.0610	0.0000	
	15	0.8697	0.8696	0.0000	1.0621	1.0610	0.0000	
	Throughput		$\theta_{Sim} = 14.1233, \theta_{Analytic} = 14.2439$			$\theta_{Sim} = 14.1009, \theta_{Analytic} = 14.2293$		

**Table 5.** Flow percentage from source corridors to exit corridors.

Source Corridor	$\lambda$	Exit Corridor	Percentage	New Weighted Travel Distance	New Optimal Arrival Rate		
					$\lambda$	$\theta$	$p(c)$
6	1.4900	1	100.00	5.0354	6.0700	6.0130	0.0094
		2	0.00				
7	5.7400	2	44.95	1.7813	14.4400	14.2799	0.0111
		3a	55.05				
8	2.5800	3a	0.00	5.0354	4.3600	4.2630	0.0223
		4	100.00				
9	1.4900	4	0.00	4.1270	4.4400	4.3654	0.0168
		5	100.00				
10	2.6000	3a	0.00	4.9500	3.6800	3.6230	0.0155
		12	50.00				
		13	50.00				
11	6.2100	12	0.00	4.0950	3.4500	3.3781	0.0208
		13	0.00				
		14	68.43				
		15	31.56				

probability. The new optimal arrival rates to the source corridors are as in Table 6. Observe that the new optimal rate of each source corridor except corridor 11 is within its allowable range. For corridor 11, its optimal arrival rate which is 3.4500 is out of the range of [4.2500, 6.8600]. This new right hand side value violates one of the problem's constraints. Thus, the problem has to be re-solved by changing the optimal arrival rate of source corridor 11 from the current value of

6.2100–3.4500 (which is the optimal value of routing pedestrians to corridors 14 and 15; i.e.  $P_{11} = 0$ ) while keeping other arrival rates to source corridors 6, 7, 8, 9 and 10.

Re-solving the problem yields  $x_{S \rightarrow 6} = 1.4900$ ,  $x_{S \rightarrow 7} = 5.7400$ ,  $x_{S \rightarrow 8} = 2.5800$ ,  $x_{S \rightarrow 9} = 1.4900$ ,  $x_{S \rightarrow 10} = 2.6000$  and  $x_{S \rightarrow 11} = 3.4500$  and the total maximum flow of 17.3500, with the conditions that  $x_{6 \rightarrow 1} = 1.4900$ ,  $x_{S6 \rightarrow 2} = 0.0000$ ,  $x_{7 \rightarrow 2} = 2.5800$ ,

**Table 6.** Sensitivity analysis for source corridors.

Source Corridor	Current Value	Slack or Surplus	Allowable Decrease	Allowable Increase	Allowable Range	Dual Price
6	14.1800	12.6900	12.6900	Infinity	[1.4900, $\infty$ )	0.0000
7	14.4600	8.7200	8.7200	Infinity	[5.7400, $\infty$ )	0.0000
8	10.1100	7.5300	7.5300	Infinity	[2.5800, $\infty$ )	0.0000
9	10.2900	8.8000	8.8000	Infinity	[1.4900, $\infty$ )	0.0000
10	6.7500	4.1500	4.1500	Infinity	[2.6000, $\infty$ )	0.0000
11	6.2100	0.0000	1.9600	0.6500	[4.2500, 6.8600]	1.0000

**Table 7.** Analytical results for the second routing policy.

Type	Corridor	Model	Flexible Arrival Rate			Same Arrival Rate for Corridors 6, 7, 8 and 9		
			$\lambda$	$\theta$	$p(c)$	$\lambda$	$\theta$	$p(c)$
Source	6	<i>real_analytic</i>	1.4900	1.4900	0.0000	2.8250	2.8250	0.0000
		<i>real_sim</i>		1.4915	0.0000		2.8241	0.0000
	7	<i>real_analytic</i>	5.7400	5.7400	0.0000	2.8250	2.8250	0.0000
		<i>real_sim</i>		5.7335	0.0000		2.8274	0.0000
	8	<i>real_analytic</i>	2.5800	2.5800	0.0000	2.8250	2.8250	0.0000
		<i>real_sim</i>		2.5830	0.0000		2.5805	0.0000
	9	<i>real_analytic</i>	1.4900	1.4900	0.0000	2.8250	2.8250	0.0000
		<i>real_sim</i>		1.4898	0.0000		2.8259	0.0000
	10	<i>real_analytic</i>	2.6000	2.6000	0.0000	2.6000	2.6000	0.0000
		<i>real_sim</i>		2.5999	0.0000		2.6008	0.0000
	11	<i>real_analytic</i>	3.4500	3.3781	0.0208	3.4500	3.3781	0.0208
<i>real_sim</i>			2.6986	0.2155		2.6592	0.2284	
Intermediate	3a	<i>real_analytic</i>	3.1599	3.0614	0.0312	1.4899	1.4478	0.0283
		<i>real_sim</i>		2.4299	0.1790		3.0246	2.3568
Exit	1	<i>real_analytic</i>	1.4900	1.4478	0.0283	2.5801	2.5077	0.0280
		<i>real_sim</i>		1.1417	0.2327		1.4894	1.1327
	2	<i>real_analytic</i>	2.5801	2.5077	0.0281	3.1600	3.0614	0.0312
		<i>real_sim</i>		1.8762	0.3220		2.5807	1.9038
	3b	<i>real_analytic</i>	1.5307	1.5020	0.0187	1.5307	1.5020	0.0187
		<i>real_sim</i>		1.2150	0.0000		1.1784	1.1784
	3c	<i>real_analytic</i>	1.5307	1.5020	0.0187	1.5307	1.5020	0.0187
		<i>real_sim</i>		1.2150	0.0000		1.1784	1.1783
	4	<i>real_analytic</i>	2.5800	2.4973	0.0321	2.5801	2.4973	0.0321
		<i>real_sim</i>		1.8922	0.2665		2.4727	1.9650
	5	<i>real_analytic</i>	1.4900	1.4478	0.0283	1.5221	1.4364	0.0563
		<i>real_sim</i>		1.1323	0.2382		1.4904	1.1374
	12	<i>real_analytic</i>	1.3000	1.2792	0.0160	1.3000	1.2792	0.0160
		<i>real_sim</i>		1.2986	0.0000		1.3004	1.2991
	13	<i>real_analytic</i>	1.3000	1.2792	0.0160	1.3000	1.2792	0.0160
		<i>real_sim</i>		1.2986	0.0000		1.3004	1.2991
	14	<i>real_analytic</i>	1.6891	1.6891	0.0000	1.6891	1.6891	0.0000
		<i>real_sim</i>		1.3493	1.3486	0.0000	1.3296	1.3288
	15	<i>real_analytic</i>	1.6891	1.6891	0.0000	1.6891	1.6891	0.0000
		<i>real_sim</i>		1.3493	1.3485	0.0000	1.3296	1.3288
Throughput	$\theta_{Analytic} = 16.8412, \theta_{Sim} = 13.7665$					$\theta_{Analytic} = 16.8298, \theta_{Sim} = 13.7514$		

$x_{7 \rightarrow 3a} = 3.1600, x_{8 \rightarrow 3a} = 0.0000, x_{8 \rightarrow 4} = 2.5800, x_{9 \rightarrow 4} = 0.0000, x_{9 \rightarrow 5} = 1.4900, x_{10 \rightarrow 3a} = 0.0000, x_{10 \rightarrow 12} = 1.3000$  and  $x_{S10 \rightarrow 13} = 1.3000, x_{11 \rightarrow 12} = 0.0000, x_{11 \rightarrow 13} = 0.0000, x_{11 \rightarrow 14} = 1.7200$  and  $x_{11 \rightarrow 15} = 1.7200$ . Based on the flow,  $P_6 = 1.000, P_7 = 0.4495, P_8 = 0.0000, P_9 = 0.0000, P_{10} = 0.0000$  and  $P_{11} = 0.0000$ . All the flow values of the source corridors are now within their allowable ranges. Inputting these values into *real\_analytic* yields the overall throughput of 16.8412. The detailed performance measures of the corridors based on rates are shown in Table 7. Observe that the main discrepancy of the overall throughput between the two models is much influenced by the throughputs of corridors 11, 3a, 1, 2, 4 and 5. As previous reasons, the optimal arrival rates to the corridors based on the simulation model are much smaller compared to the analytical model.

For the simulation model,  $x_{S \rightarrow 6} = 1.3473, x_{S \rightarrow 7} = 5.0081, x_{S \rightarrow 8} = 2.300, x_{S \rightarrow 9} = 1.3473, x_{S \rightarrow 10} = 2.5234$  and  $x_{S \rightarrow 11} = 3.2900$  generate the maximum

throughput of 15.8161, with the conditions that  $x_{6 \rightarrow 1} = 1.3400, x_{S6 \rightarrow 2} = 0.0000, x_{7 \rightarrow 2} = 2.3801, x_{7 \rightarrow 3a} = 2.7000, x_{8 \rightarrow 3a} = 0.0000, x_{8 \rightarrow 4} = 2.3000, x_{9 \rightarrow 4} = 0.0000, x_{9 \rightarrow 5} = 1.3473, x_{10 \rightarrow 3a} = 0.0000, x_{10 \rightarrow 12} = 1.2617$  and  $x_{10 \rightarrow 13} = 1.2617, x_{11 \rightarrow 12} = 0.0000, x_{11 \rightarrow 13} = 0.0000, x_{11 \rightarrow 14} = 1.6450$  and  $x_{11 \rightarrow 15} = 1.6450$ . Thus,  $P_6 = 1.000, P_7 = 0.4608, P_8 = P_9 = P_{10} = P_{11} = 0.0000$ . The detailed results of the simulation model and the throughput comparison with the analytical model for these values are shown in Table 8. If we impose  $x_{S \rightarrow 6} = x_{S \rightarrow 7} = x_{S \rightarrow 8} = x_{S \rightarrow 9}$ , then  $x_{S \rightarrow 6} = x_{S \rightarrow 7} = x_{S \rightarrow 8} = x_{S \rightarrow 9} = 2.5007, x_{S \rightarrow 10} = 2.5234$  and  $x_{S \rightarrow 11} = 3.2900$  generate the maximum throughput of 15.0041 with the conditions that  $x_{6 \rightarrow 1} = 1.3473, x_{6 \rightarrow 2} = 1.1534, x_{7 \rightarrow 2} = 1.1547, x_{7 \rightarrow 3a} = 1.3460, x_{8 \rightarrow 3a} = 1.3541, x_{8 \rightarrow 4} = 1.1466, x_{9 \rightarrow 4} = 1.1534, x_{9 \rightarrow 5} = 1.3473, x_{10 \rightarrow 3a} = 0.0000, x_{10 \rightarrow 12} = 1.2617$  and  $x_{S10 \rightarrow 13} = 1.2617, x_{11 \rightarrow 12} = 0.0000, x_{11 \rightarrow 13} = 0.0000, x_{11 \rightarrow 14} = 1.6450$  and  $x_{11 \rightarrow 15} = 1.6450$ . Thus,  $P_6 = 0.5388, P_7 = 0.4618, P_8 = 0.5415, P_9 = 0.4612, P_{10} = 0.0000$

**Table 8.** Simulation results for the second routing policy.

Type	Corridor	Flexible Arrival Rate			Same Arrival Rate for Corridors 6, 7, 8 and 9		
		$\lambda$	$\theta$	$p(c)$	$\lambda$	$\theta$	$p(c)$
Source	6	1.3473	1.3475	0.0000	2.5007	2.5008	0.0000
	7	5.0081	5.0082	0.0000	2.5007	2.5011	0.0000
	8	2.3000	2.2996	0.0000	2.5007	2.5001	0.0000
	9	1.3473	1.3471	0.0000	2.5007	2.5016	0.0000
	10	2.5234	2.5250	0.0000	2.5234	2.5251	0.0000
Intermediate	11	3.2900	3.0326	0.0768	3.2900	3.0897	0.0606
	3a	2.6999	2.6294	0.0264	2.6999	2.6186	0.0302
Exit	1	1.3475	1.3065	0.0296	1.3474	1.2991	0.0348
	2	2.3083	2.2506	0.0238	2.3084	2.2380	0.0296
	3b	1.3147	1.3146	0.0000	1.3093	1.3092	0.0000
	3c	1.3147	1.3146	0.0000	1.3093	1.3092	0.0000
	4	2.2996	2.1077	0.0827	2.3000	2.1547	0.0624
	5	1.3471	1.2859	0.0444	1.3479	1.2958	0.0377
	12	1.2625	1.2613	0.0000	1.2626	1.2614	0.0000
	13	1.2625	1.2613	0.0000	1.2626	1.2614	0.0000
	14	1.5163	1.5155	0.0000	1.5449	1.5440	0.0000
	15	1.5163	1.5154	0.0000	1.5449	1.5440	0.0000
Throughput		$\theta_{Sim} = 15.1334, \theta_{Analytic} = 15.7904$			$\theta_{Sim} = 15.2168, \theta_{Analytic} = 15.7906$		

**Table 9.** Ranking of the best routing policy.

Model	Policy	Throughput		Arrival Rate
		Analytic	Simulation	
Analytical	Second Routing Policy	16.8412	13.7665	$x_{S \rightarrow 6} = 1.4900, x_{S \rightarrow 7} = 5.7400, x_{S \rightarrow 8} = 2.5800,$ $x_{S \rightarrow 9} = 1.4900, x_{S \rightarrow 10} = 2.6000$ and $x_{S \rightarrow 11} = 3.4500$ with $P_6 = 1.000, P_7 = 0.4495, P_8 = 0.0000,$ $P_9 = 0.0000, P_{10} = 0.0000$ and $P_{11} = 0.0000$
	First Routing Policy (Alternative)	15.9034	13.1181	$x_{S \rightarrow 6} = 1.0200, x_{S \rightarrow 7} = 4.1400, x_{S \rightarrow 8} = 2.1800,$ $x_{S \rightarrow 9} = 2.9800, x_{S \rightarrow 10} = 2.6000$ and $x_{S \rightarrow 11} = 3.4500$
	First Routing	15.1672	13.3806	$x_{S \rightarrow 6} = x_{S \rightarrow 7} = x_{S \rightarrow 8} = x_{S \rightarrow 9} = 2.5800,$ $x_{S \rightarrow 10} = 1.1600$ and $x_{S \rightarrow 11} = 4.0400$
Simulation	Second Routing Policy	15.7906	15.2168	$x_{S \rightarrow 6} = x_{S \rightarrow 7} = x_{S \rightarrow 8} = x_{S \rightarrow 9} = 2.5007,$ $x_{S \rightarrow 10} = 2.5234$ and $x_{S \rightarrow 11} = 3.2900$ with $P_6 = 0.5388, P_7 = 0.4618, P_8 = 0.5415, P_9 = 0.4612,$ $P_{10} = 0.0000$ and $P_{11} = 0.0000$
	First Routing Policy (Alternative)	15.0046	14.6011	$x_{S \rightarrow 6} = 1.1216, x_{S \rightarrow 7} = 3.4946, x_{S \rightarrow 8} = 1.9054,$ $x_{S \rightarrow 9} = 2.6946, x_{S \rightarrow 10} = 2.5234$ and $x_{S \rightarrow 11} = 3.2900$
	First Routing	14.2439	14.1233	$x_{S \rightarrow 6} = 2.6946, x_{S \rightarrow 7} = 1.9216, x_{S \rightarrow 8} = 1.9054,$ $x_{S \rightarrow 9} = 2.6946, x_{S \rightarrow 10} = 1.5730$ and $x_{S \rightarrow 11} = 3.4738$

and  $P_{11} = 0.0000$ . The detailed performance measures for each corridor based on these values are as in Table 8. For these two sets of values, there are very small congestions along all routes.

### 5.3. Recommendation

The detailed ranking of the policies is shown in Table 9. The policies are ranked based on the highest throughput generated by the analytical and simulation models. Notice that we also consider an alternative to the first policy implementing the same logic considered in the first policy. The only difference is that we force all pedestrians in corridor 11 to only travel to corridors 14 or 15 and that in corridor 10 to only travel in a single direction to corridors 12 or 13. As observed, the second policy is the best policy and

should thus be chosen for vacating pedestrians. If the vacating processes implement the arrival rates and routing probabilities shown in the first row of Table 9, *real\_analytic* then generates the overall throughput of 16.8412 peds/s. However, for these values, *real\_sim* only generates the throughput of 13.7665 peds/s.

The maximum throughput which can be achieved by *real\_sim* based on the second policy is 15.2168 peds/s. For the suggested arrival rates and routing probabilities (see the fourth row of Table 9), the throughput of *real\_analytic* is 15.7906 peds/s and the flow is smooth in all routes. Since there is a small throughput discrepancy between the two models, the flow control based on this strategy is the best option. For vacating processes, pedestrians should thus be flowed to enter corridors 6, 7, 8 and 9 with the arrival rates of 2.5007 peds/s. 54% of pedestrians of

corridor 6 ( $P_6 = 0.5388$ ) should travel to corridor 1, 46% of pedestrians of corridor 7 ( $P_7 = 0.4618$ ) should travel to corridor 2, 54% of pedestrians of corridor 8 ( $P_8 = 0.5415$ ) should travel to corridor 3a and 46% of pedestrians of corridor 9 ( $P_9 = 0.4612$ ) should travel to corridor 4. For corridor 10, pedestrians should be flowed to the corridor with 2.5234 peds/s and forced to only travel to corridors 11 and 13 to exit the hall. For corridor 11, the pedestrians should be flowed to the corridor with 3.2900 peds/s and forced to only travel corridors 14 and 15 to exit the hall.

The time to vacate all of the 1338 occupants from the hall is approximately  $1338/15.2168 \approx 88$  s. This is the optimal time to vacate the occupants through the ten exit corridors which can only be achieved if the optimal arrival rates and routing probabilities are implemented under a normal condition. Lower arrival rates reduce the overall throughput at the end. Higher arrival rates meanwhile increase the blocking probabilities along the routes instead of improving the overall throughput at the end.

Observe that in many cases of the computational experiments, analytical results are very close to simulation results. The results reflect some essential relationships between both models. First, the analytical model provides a static approximation effect of pedestrian density on the state of a network while the simulation model imitates pedestrians' behaviour and interactions while flowing in the network. Simulation is thus an important tool for getting insight into the dynamic processes of the state-dependent flow. Second, the analytical model measures the performance of the network using relevant  $M/G/C/C$  mathematical expressions while the simulation model validates the analytical expressions. Simulation is thus an effective tool for showing the accuracy of the various considered settings or configurations. Third, the analytical model measures the performance based on relevant assumptions (e.g. exponential inter-arrival time) while the simulation predicts the performance based

on designated flow logic. Simulation is thus an indispensable tool for evaluating further effect of various scenarios on the network performance over the analytical model. This includes the impact of changing arrival rates from an exponential distribution to other distributions (e.g. triangular or normal) or closing relevant sink nodes with finite capacities after a point of time on the throughput.

A further important aspect of the models is the implementation of its policy. The policy is very specific in terms of its optimal arrival rates and turning proportions or route fractions. How can the policy be applied in practice? In reality, we cannot control the flow to exactly match the suggested values. The flow in all corridors should thus be properly controlled within the acceptable ranges of the suggested values to optimise the overall flow. To measure the arrival rates to source nodes, a sensor computing the arrival rates through light array as proposed in previous studies (Shende, 2008; Shende et al., 2013) can be used. Route choices can meanwhile be enforced by providing relevant persons at each intersection who will guide the incoming pedestrians to relevant downstream directions. Pedestrians can also be recommended to use or not to use relevant corridors during their movement using loudspeakers.

### 5.4. Verification of the proposed policies

Thus far the proposed policies were analysed using an  $M/G/C/C$  model. In literature, there are other state dependent queuing models which extensively analyse and relate pedestrian speed and density in a constrained space based on various sets of secondary data of pedestrian speed. The models include Green-shields (1935), Greenberg (1959), Underwood (1960), Drake et al. (1965), Pipes-Munjaj (Pipes, 1967), Drew (1968), Northwestern (May, 1990), Modified Green-shields (Jayakrishnan et al., 1995),  $M/G/C/C$  linear (Yuhaski & Smith, 1989) and logistic speed-density

**Table 10.** Speed-density models.

Model	Function	Optimal $\rho$	Optimal $q$
Underwood	$v(\rho) = v_f e^{-\frac{\rho}{\rho_m}}$	$\rho_{opt} = \rho_m$	$q_{opt} = \frac{\rho_m v_f}{e}$
Pipes-Munjaj	$v(\rho) = v_f \left[ 1 - \left( \frac{\rho}{\rho_m} \right)^n \right]$	$\rho_{opt} = \left[ \frac{\rho_m^n}{n+1} \right]^{\frac{1}{n}}$	$q_{opt} = \left[ \frac{n}{n+1} \right] v_f \left[ \frac{\rho_m^n}{n+1} \right]^{\frac{1}{n}}$
Drew (1968)	$v(\rho) = v_f \left[ 1 - \left( \frac{\rho}{\rho_m} \right)^{n+\frac{1}{2}} \right]$	$\rho_{opt} = \left[ \frac{2\rho_m^{n+\frac{1}{2}}}{2n+3} \right]^{\frac{2}{2n+1}}$	$q_{opt} = v_f \left[ \frac{2\rho_m^{n+\frac{1}{2}}}{2n+3} \right]^{\frac{2}{2n+1}} \left[ \frac{2n+1}{2n+3} \right]$
$M/G/C/C$ Linear	$v(\rho) = \frac{v_f}{\rho_m} (\rho_m + 1 - \rho)$	$\rho_{opt} = \frac{\rho_m + 1}{2}$	$q_{opt} = \frac{v_f}{4\rho_m} (\rho_m + 1)^2$

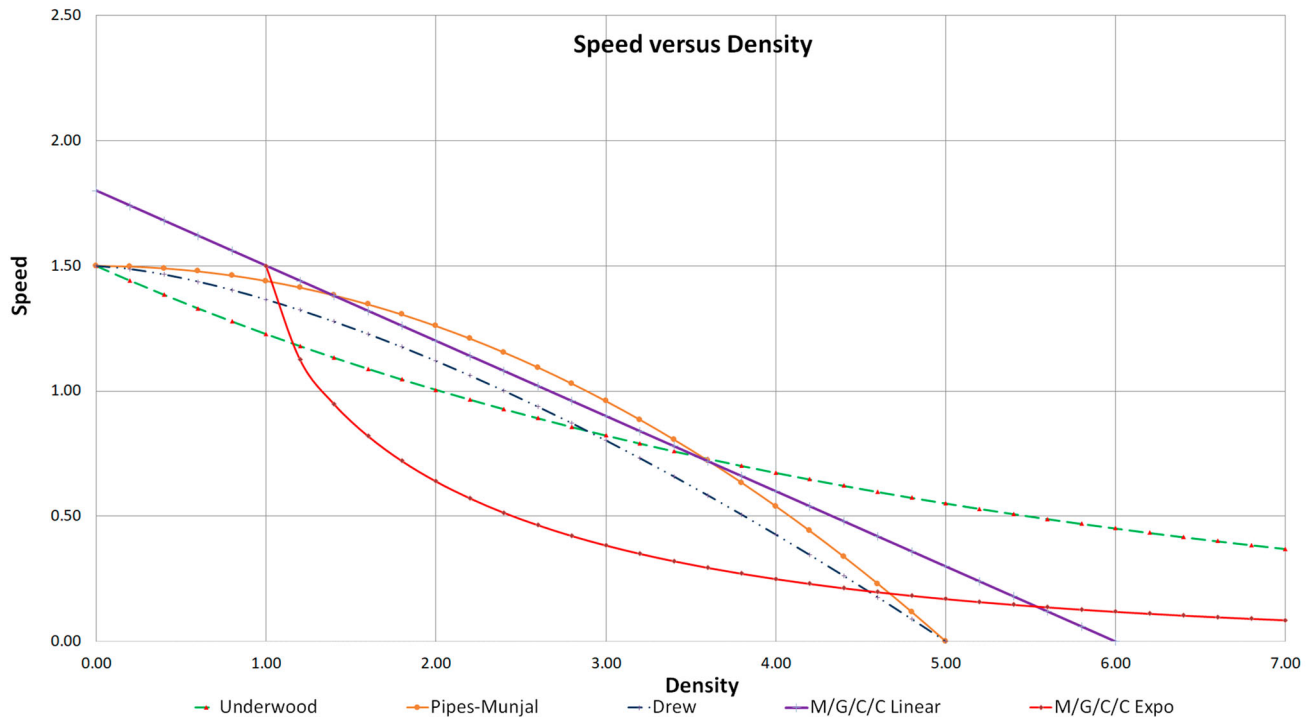


Figure 8. Speed-density relationships.

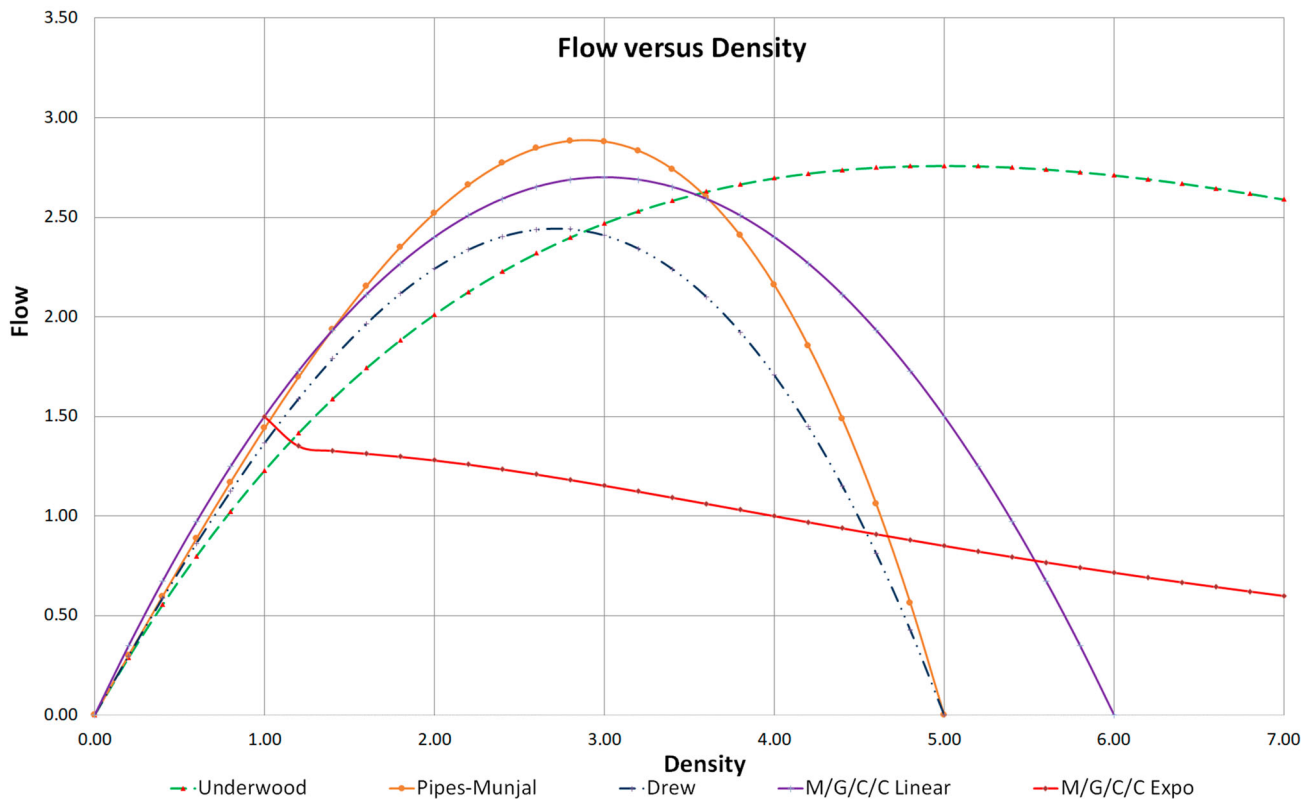


Figure 9. Flow-density relationships.



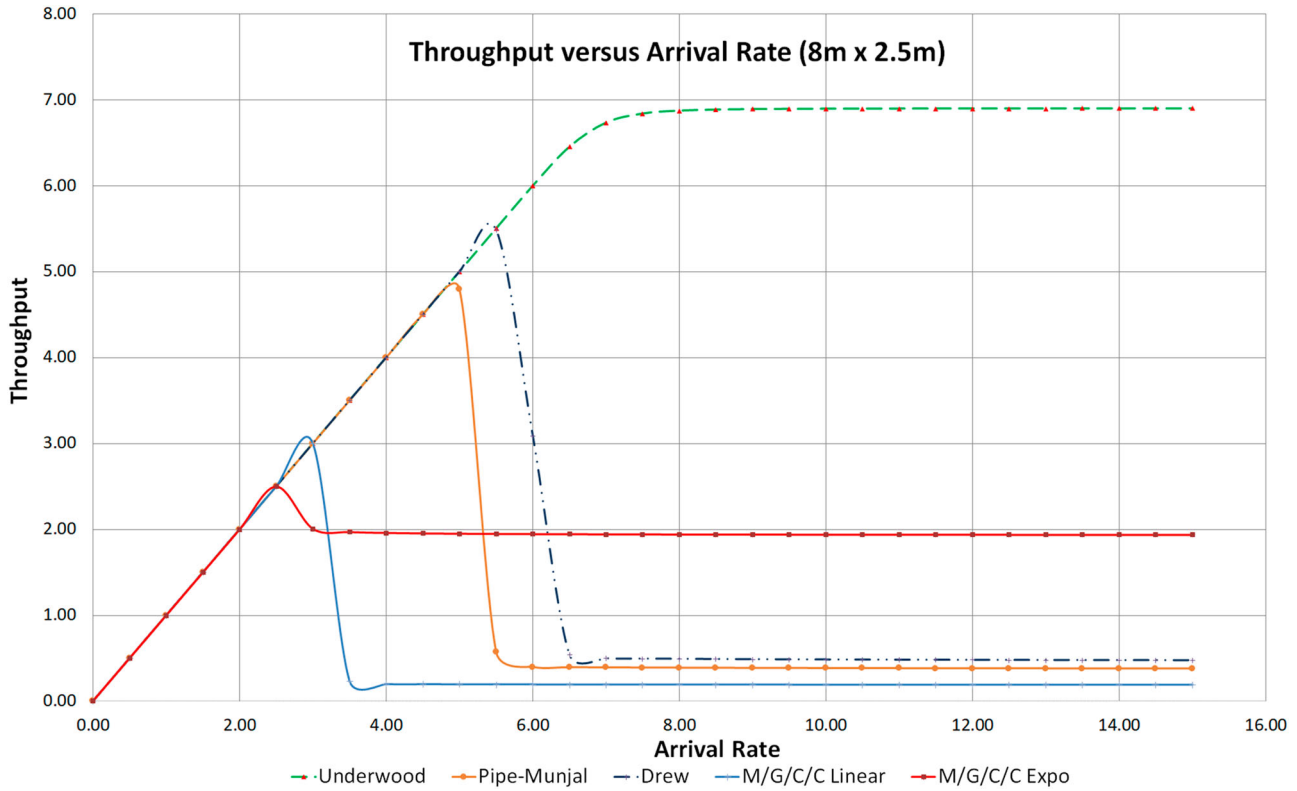


Figure 10. Throughput-arrival rate relationships for an 8m × 2.5m space.

Table 11. Optimal λ and its impact on the performance measures of an 8m × 2.5m space.

Model	λ	θ	P <sub>C</sub>	E(N)	E(T)
Underwood	8.1455	6.8758	0.1559	94.7697	13.783
Pipes-Munjial (n = 2)	3.4105	3.3684	0.0123	19.9957	5.9362
Drew (n = 1)	3.8515	3.8027	0.0127	22.0694	5.8035
M/G/C/C Linear	3.1184	3.0787	0.0127	22.2828	7.2377
M/G/C/C Exponential	2.6983	2.6608	0.0139	28.9942	10.8966

(Wang et al., 2011) models. Using these models to further verify the proposed policies to see how the hall throughput varies across them is thus crucial. The functions, derived optimal density and optimal flow of some of the models are shown in Table 10. Note that  $v$  is the average traffic speed,  $v_f$  is the free flow

(maximum) speed; i.e. the speed of a lone pedestrian or vehicle,  $\rho$  is the traffic density; i.e. the number of pedestrians or vehicles per unit area,  $\rho_m$  is the maximum or critical density at which a traffic jam will occur and the speed is near to zero and  $q = \rho \cdot v$  is the flow through the area. Setting  $v_f = 1.5$  m/s and  $\rho_m = 5$  peds/m<sup>2</sup>, the graphical pedestrian speed-density and flow-density for a 1 m × 1 m space are respectively plotted in Figures 8 and 9. Based on the speed-density relationships, the performance of the space can be measured using Equations (2) and (3). For example, the performance of an 8 m × 2.5 m space in terms of how arrival rates effect its throughput is plotted in Figure 10. The optimal arrival rate,  $\lambda_{opt}$  and its impact

Table 12. The throughput of the hall based on various speed-density models.

Routing Policy	Analytical	Simulation
	$x_{S \rightarrow 6} = 1.4900, x_{S \rightarrow 7} = 5.7400, x_{S \rightarrow 8} = 2.5800,$ $x_{S \rightarrow 9} = 1.4900, x_{S \rightarrow 10} = 2.6000$ and $x_{S \rightarrow 11} = 3.4500$ with $P_6 = 1.000, P_7 = 0.4495, P_8 = 0.0000,$ $P_9 = 0.0000, P_{10} = 0.0000$ and $P_{11} = 0.0000$	$x_{S \rightarrow 6} = x_{S \rightarrow 7} = x_{S \rightarrow 8} = x_{S \rightarrow 9} = 2.5007,$ $x_{S \rightarrow 10} = 2.5234$ and $x_{S \rightarrow 11} = 3.2900$ with $P_6 = 0.5388,$ $P_7 = 0.4618, P_8 = 0.5415, P_9 = 0.4612, P_{10} = 0.0000$ and $P_{11} = 0.0000$
Model	θ	
Underwood	17.3500	15.8162
Pipes-Munjial (n = 2)	11.9697	12.9886
Drew (n = 1)	14.1554	13.1146
M/G/C/C Linear	17.3490	15.8161
M/G/C/C Exponential	16.8412	15.7906

on the performance of the space based on the various speed-density models are meanwhile shown Table 11.

Using the various speed-density models, the best routing policy of the analytical and simulation models based on  $M/G/C/C$  exponential was further verified. The speed-density models generate different hall throughputs as shown in Table 12. As observed, the hall throughputs based on the best analytical routing policy are between 11.9697 and 17.3500 while the throughputs based on the best simulation routing policy are between 12.9886 and 15.8162 for the various speed-density models. For both routing policies, the Pipes-Munjial model generates the lowest hall throughput while the Underwood model generates the highest hall throughput compared to the other models.

## 6. Conclusion

The throughput of a network corresponding to its pedestrian exit time can be optimised by maximising its pedestrian flow. This paper proposes a framework for optimising pedestrian flow in a complex topological network with multiple entrances (along its source nodes) and exits using the combination of  $M/G/C/C$  analytical and simulation models and the network flow model. The  $M/G/C/C$  models replicate the speed-density relationship of pedestrians in all available nodes in the network. The network flow model meanwhile derives the optimal flow in the source nodes and routing probabilities of pedestrians to the downstream nodes maximising the network's throughput.

Implementing the framework on the DTSP and comparing its quantitative results with other considered routing policies shows that the throughput of the hall can be maximised if the arrival rates of pedestrians to the available entrances and their flow directions are controlled at relevant levels. This optimal policy also guarantees that the blocking probabilities along all available routes are minimised. The framework can be used to design a routing policy for any state dependent queuing networks; e.g. pedestrian traffic networks and vehicular traffic networks to efficiently flow entities from the network and to support the evacuation process during emergency cases in order to reduce the risks of injuries and death.

## Acknowledgments

This study was supported by the Hajj Research Cluster, USM No. 203.PTS.6720008, Ministry of Higher Education, Malaysia.

We wish to thank the ministry for the financial support. The funder had no role in study design, data collection and analysis, decision to publish, or preparation of the manuscript.

## Disclosure statement

No potential conflict of interest was reported by the author(s).

## Funding

This study was supported by the Hajj Research Cluster, USM No. 203.PTS.6720008, Ministry of Higher Education, Malaysia.

## Notes on contributors

*Ruzelan Khalid* is a senior lecturer in Decision Science at Universiti Utara Malaysia, Malaysia. He obtained his Ph.D. in Computer Science from University of Canterbury, New Zealand. His research interests include Discrete Event Simulation, Component-Based Framework and Queuing Networks.

*Mohd Kamal Mohd Nawawi* is an associate professor in Decision Science at Universiti Utara Malaysia, Malaysia. He received his Ph.D. in Manufacturing Engineering (Lean Manufacturing & Operational Research) from University of Bradford, United Kingdom. His research interests include Discrete Event Simulation, Lean Manufacturing and Knowledge Based System.

*Luthful A. Kawsar* a professor at Department of Statistics, Shahjalal University of Science and Technology, Bangladesh. He received his Ph.D. in Statistics from Universiti Sains Malaysia, Malaysia. His research interests include Mathematical Modeling, Queuing networks and Operations Research.


*Noraida A. Ghani* is an associate professor at the School of Distance Education, Universiti Sains Malaysia. She was awarded a Doctor of Science in Operations Research from the George Washington University, Washington, D.C. Her research interests include emergency medical services, stochastic modeling in health sector and pedestrian and crowd.

*Anton A. Kamil* is a professor at the Faculty of Economics, Administrative and Social Sciences, Istanbul Gelisim University, Turkey. He received his PhD from University of Economics (VSE), Prague, Czech Republic. His research interests include stochastic frontier analysis and financial mathematics.

*Adli Mustafa* is a senior lecturer at the School of Mathematical Sciences, Universiti Sains Malaysia. He received his PhD from the National University of Singapore. His research interests include data envelopment analysis, network flows, integer programming and transportation.

## ORCID

*Ruzelan Khalid*  <http://orcid.org/0000-0002-4283-0737>

*Mohd Kamal Mohd Nawawi*  <http://orcid.org/0000-0003-4447-9941>

Luthful A. Kawsar  <http://orcid.org/0000-0002-8010-6379>  
 Anton A. Kamil  <http://orcid.org/0000-0001-5410-812X>  
 Adli Mustafa  <http://orcid.org/0000-0003-0989-674X>

## References

- Antonini, G., Bierlaire, M., & Weber, M. (2006). Discrete choice models of pedestrian walking behavior. *Transportation Research Part B: Methodological*, 40(8), 667–687. <https://doi.org/10.1016/j.trb.2005.09.006>
- Asano, M., Sumalee, A., Kuwahara, M., & Tanaka, S. (2007). Dynamic cell transmission-based pedestrian model with multidirectional flows and strategic route choices. *Transportation Research Record: Journal of the Transportation Research Board*, 2039(1), 42–49. <https://doi.org/10.3141/2039-05>
- Blue, V. J., & Adler, J. L. (2001). Cellular automata microsimulation for modeling bi-directional pedestrian walkways. *Transportation Research Part B: Methodological*, 35(3), 293–312. [https://doi.org/10.1016/S0191-2615\(99\)00052-1](https://doi.org/10.1016/S0191-2615(99)00052-1)
- Burstedde, C., Klauck, K., Schadschneider, A., & Zittartz, J. (2001). Simulation of pedestrian dynamics using a two-dimensional cellular automaton. *Physica A: Statistical Mechanics and its Applications*, 295(3-4), 507–525. [https://doi.org/10.1016/S0378-4371\(01\)00141-8](https://doi.org/10.1016/S0378-4371(01)00141-8)
- Campos, V., Bandeira, R., & Bandeira, A. (2012). A method for evacuation route planning in disaster situations. *Procedia - Social and Behavioral Sciences*, 54, 503–512. <https://doi.org/10.1016/j.sbspro.2012.09.768>
- Cao, S., Fu, L., & Song, W. (2018). Exit selection and pedestrian movement in a room with two exits under fire emergency. *Applied Mathematics and Computation*, 332, 136–147. <https://doi.org/10.1016/j.amc.2018.03.048>
- Cao, S., Seyfried, A., Zhang, J., Holl, S., & Song, W. (2017). Fundamental diagrams for multidirectional pedestrian flows. *Journal of Statistical Mechanics: Theory and Experiment*, 95(3). Article 033404. <https://doi.org/10.1088/1742-5468/aa620d>
- Cao, S., Song, W., Lv, W., & Fang, Z. (2015). A multi-grid model for pedestrian evacuation in a room without visibility. *Physica A: Statistical Mechanics and its Applications*, 436, 45–61. <https://doi.org/10.1016/j.physa.2015.05.019>
- Cao, S., Zhang, J., Salden, D., Ma, J., Shi, C., & Zhang, R. (2016). Pedestrian dynamics in single-file movement of crowd with different age compositions. *Physical Review E*, 94(1), Article 012312. <https://doi.org/10.1103/PhysRevE.94.012312>
- Chalmet, L. G., Francis, R. L., & Saunders, P. B. (1982). Network models for building evacuation. *Fire Technology*, 18(1), 90–113. <https://doi.org/10.1007/BF02993491>
- Cheah, J. (1990). State dependent queueing models [Master thesis, Department of Industrial Engineering and Operations Research, University of Massachusetts, Amherst, MA].
- Cheah, J., & Smith, J. M. (1994). Generalized M/G/C/C state dependent queueing models and pedestrian traffic flows. *Queueing Systems*, 15(1), 365–386. <https://doi.org/10.1007/BF01189246>
- Chen, C. C., & Chou, C. S. (2009). Modeling and performance assessment of a transit-based evacuation plan within a contraflow simulation environment. *Transportation Research Record: Journal of the Transportation Research Board*, 2091(1), 40–50. <https://doi.org/10.3141/2091-05>
- Cova, T. J., & Johnson, J. P. (2003). A network flow model for lane-based evacuation routing. *Transportation Research Part A: Policy and Practice*, 37(7), 579–604. [https://doi.org/10.1016/S0965-8564\(03\)00007-7](https://doi.org/10.1016/S0965-8564(03)00007-7)
- Cruz, F. R. B., Kendall, G., While, L., Duarte, A. R., & Brito, N. L. C. (2012). Throughput maximization of queueing networks with simultaneous minimization of service rates and buffers. *Mathematical Problems in Engineering*, 2012, 1–19. <https://doi.org/10.1155/2012/692593>
- Cruz, F. R. B., & Smith, J. M. (2007). Approximate analysis of M/G/c state-dependent queueing networks. *Computers & Operations Research*, 34(8), 2332–2344. <https://doi.org/10.1016/j.cor.2005.09.006>
- Cruz, F. R. B., Smith, J. M., & Medeiros, R. O. (2005). An M/G/C/C state dependent network simulation model. *Computers & Operations Research*, 32(4), 919–941. <https://doi.org/10.1016/j.cor.2003.09.006>
- Cruz, F. R. B., van Woensel, T., MacGregor Smith, J., & Lieckens, K. (2010). On the system optimum of traffic assignment in state-dependent queueing networks. *European Journal of Operational Research*, 201(1), 183–193. <https://doi.org/10.1016/j.ejor.2009.03.006>
- Cuesta, A., Abreu, O., Balboa, A., & Alvear, D. (2017). Real-time evacuation route selection methodology for complex buildings. *Fire Safety Journal*, 91, 947–954. <https://doi.org/10.1016/j.firesaf.2017.04.011>
- Drake, J. S., Schofer, J. L., & May, A. D. (1965). A statistical analysis of speed density hypothesis. *Highway Research Record*, 154, 53–87. <https://trid.trb.org/view.aspx?id=693312>
- Drew, D. R. (1968). *Traffic flow theory and control*. McGraw-Hill.
- Fang, Z., Li, Q., Li, Q., Han, L. D., & Wang, D. (2011). A proposed pedestrian waiting-time model for improving space time use efficiency in stadium evacuation scenarios. *Building and Environment*, 46(9), 1774–1784. <https://doi.org/10.1016/j.buildenv.2011.02.005>
- Fang, Z., Zong, X., Li, Q., Li, Q., & Xiong, S. (2011). Hierarchical multi-objective evacuation routing in stadium using ant colony optimization approach. *Journal of Transport Geography*, 19(3), 443–451. <https://doi.org/10.1016/j.jtrangeo.2010.10.001>
- Farahani, M., Chaharsooghi, M., Woensel, S. K., & Veelenturf, T. V., & P, L. (2018). Capacitated network-flow approach to the evacuation-location problem. *Computers & Industrial Engineering*, 115, 407–426. <https://doi.org/10.1016/j.cie.2017.11.026>
- Foot, N. I. S. (1973). Pedestrian traffic flows. *DMG-DRS Journal: Design Research and Methods: Part 2*, 7, 162–167.
- Gao, Z., Qu, Y., Li, X., Long, J., & Huang, H.-J. (2014). Simulating the dynamic escape process in large public places. *Operations Research*, 62(6), 1344–1357. <https://doi.org/10.1287/opre.2014.1312>

- Garrido, J. M. (1998). *Practical process simulation using object-oriented techniques and C++*. Artech House.
- Garrido, J. M. (2001). *Object-oriented discrete-event simulation with Java - A practical introduction*. Springer.
- Greenberg, H. (1959). An analysis of traffic flow. *Operations Research*, 7(1), 79–85. <https://doi.org/10.1287/opre.7.1.79>
- Greenshields, B. D. (1935). A study in highway capacity. *Highway Research Board Proceedings*, 14, 448–477.
- Gwynne, S., Galea, E. R., Owen, M., Lawrence, P. J., & Filippidis, L. (1999). A review of the methodologies used in the computer simulation of evacuation from the built environment. *Building and Environment*, 34(6), 741–749. [https://doi.org/10.1016/S0360-1323\(98\)00057-2](https://doi.org/10.1016/S0360-1323(98)00057-2)
- Hankin, B. D., & Wright, R. A. (1958). Passenger flow in subways. *Operational Research Quarterly*, 9(2), 81–88. <https://doi.org/10.1057/jors.1958.9>
- Hänseler, F. S., Bierlaire, M., Farooq, B., & Mühlematter, T. (2004). A macroscopic loading model for time-varying pedestrian flows in public walking areas. *Transportation Research Part B: Methodological*, 69, 60–80. <https://doi.org/10.1016/j.trb.2014.08.003>
- Hänseler, F. S., Lam, W. H. K., Bierlaire, M., Lederrey, G., & Nikolić, M. (2017). A dynamic network loading model for anisotropic and congested pedestrian flows. *Transportation Research Part B: Methodological*, 95, 149–168. <https://doi.org/10.1016/j.trb.2016.10.017>
- Helbing, D., Farkás, I. J., Molnár, P., & Vicsek, T. (2002). Simulation of pedestrian crowds in normal and evacuation situations. In M. Schreckenberg, & S. D. Sharma (Eds.), *Pedestrian and evacuation dynamics* (pp. 21–58). Springer.
- Hernández, A. L. B., Meléndez, A. M., & Huerta, A. R. (2011). Multiagent system applied to the modeling and simulation of pedestrian traffic in counterflow. *Journal of Artificial Societies and Social Simulation*, 14(3), 1–19. <https://doi.org/10.18564/jasss.1789>
- Hu, L., Jiang, Y., Zhu, J., & Chen, Y. (2015). A PH/PH(n)/C/C state-dependent queuing model for metro station corridor width design. *European Journal of Operational Research*, 240(1), 109–126. <https://doi.org/10.1016/j.ejor.2014.06.010>
- Huang, J., Zhou, F., & Xi, M. (2018). Calculation method for load capacity of urban rail transit station considering cascading failure. *Journal of Advanced Transportation*, 2018, 1–12. <https://doi.org/10.1155/2018/6318516>
- Hughes, R. L. (2002). A continuum theory for the flow of pedestrians. *Transportation Research Part B: Methodological*, 36(6), 507–535. [https://doi.org/10.1016/S0191-2615\(01\)00015-7](https://doi.org/10.1016/S0191-2615(01)00015-7)
- Jain, R., & Smith, J. M. (1997). Modeling vehicular traffic flow using M/G/C/C state dependent queueing models. *Transportation Science*, 31(4), 324–336. <https://doi.org/10.1287/trsc.31.4.324>
- Jayakrishnan, R., Tsai, W. K., & Chen, A. (1995). A dynamic traffic assignment model with traffic-flow relationships. *Transportation Research Part C: Emerging Technologies*, 3(1), 51–72. [https://doi.org/10.1016/0968-090X\(94\)00015-W](https://doi.org/10.1016/0968-090X(94)00015-W)
- Jiang, Y., Zhu, J., Hu, L., Lin, X., & Khattak, A. (2016). A G/G(n)/C/C state-dependent simulation model for metro station corridor width design. *Journal of Advanced Transportation*, 50(3), 273–295. <https://doi.org/10.1002/atr.1315>
- Kachroo, P. (2009). *Pedestrian dynamics: Mathematical theory and evacuation control*. Taylor and Francis Group.
- Kachroo, P., Al-nasur, S. J., Wadoo, S. A., & Shende, A. (2008). *Pedestrian dynamics: Feedback control of crowd evacuation*. Springer-Verlag.
- Kawsar, L. A., Ghani, N. A., Kamil, A. A., & Mustafa, A. (2013). Pedestrian performance measures of an M/G/C/C state dependent queueing network in emergency. *Journal of Applied Sciences*, 13(3), 437–443. <https://doi.org/10.3923/jas.2013.437.443>
- Kelton, W. D., Sadowski, R., & Zupick, N. (2015). *Simulation with arena* (6th ed). McGraw-Hill.
- Khalid, R., Baten, M. A., Nawawi, M. K. M., & Ishak, N. (2016). Analyzing and optimizing pedestrian flow through a topological network based on M/G/C/C and network flow approaches. *Journal of Advanced Transportation*, 50(1), 96–119. <https://doi.org/10.1002/atr.1330>
- Khalid, R., Nawawi, M. K., Kawsar, L., Ghani, N., Kamil, A., & Mustafa, A. (2016). The evaluation of pedestrians behavior using M/G/C/C analytical, weighted distance and real distance simulation models. *Discrete Event Dynamic Systems*, 26(3), 439–476. <https://doi.org/10.1007/s10626-015-0215-0>
- Khalid, R., Nawawi, M. K. M., Kawsar, L. A., Ghani, N. A., Kamil, A. A., & Mustafa, A. (2013). A discrete event simulation model for evaluating the performances of an M/G/C/C state dependent queueing system. *PLoS ONE*, 8(4), 1–9. <https://doi.org/10.1371/journal.pone.0058402>
- Khalid, M. N. A., & Yusof, U. K. (2018). Dynamic crowd evacuation approach for the emergency route planning problem: Application to case studies. *Safety Science*, 102, 263–274. <https://doi.org/10.1016/j.ssci.2017.10.024>
- Khattak, A., Yangsheng, J., & Abid, M. M. (2018). Optimal configuration of the metro rail transit station service facilities by integrated simulation-optimization method using passengers' flow fluctuation. *Arabian Journal for Science and Engineering*, 43(10), 5499–5516. <https://doi.org/10.1007/s13369-018-3194-2>
- Khattak, A., Yangsheng, J., Lu, H., & Juanxiu, Z. (2017). Width design of urban rail transit station walkway: A novel simulation-based optimization approach. *Urban Rail Transit*, 3(2), 112–127. <https://doi.org/10.1007/s40864-017-0061-5>
- Kimms, A., & Maiwald, M. (2017). An exact network flow formulation for cell-based evacuation in urban areas. *Naval Research Logistics*, 64(7), 547–555. <https://doi.org/10.1002/nav.21772>
- Kuligowski, E. D., Peacock, R. D., & Hoskins, B. L. (2005). *A review of building evacuation models*. US Department of Commerce, National Institute of Standards and Technology.
- Kunwar, B., Simini, F., & Johansson, A. (2016). Evacuation time estimate for total pedestrian evacuation using a queueing network model and volunteered geographic

- information. *Physical Review E*, 93(3), Article 032311. <https://doi.org/10.1103/PhysRevE.93.032311>
- May, A. D. (1990). *Traffic flow fundamentals*. Prentice Hall.
- Mitchell, D. H., & Smith, J. M. (2001). Topological network design of pedestrian networks. *Transportation Research Part B: Methodological*, 35(2), 107–135. [https://doi.org/10.1016/S0191-2615\(99\)00039-9](https://doi.org/10.1016/S0191-2615(99)00039-9)
- Murray-Tuite, P., & Mahmassani, H. (2003). Model of household trip-chain sequencing in emergency evacuation. *Transportation Research Record: Journal of the Transportation Research Board*, 1831(1), 21–29. <https://doi.org/10.3141/1831-03>
- Naghawi, H., & Wolshon, B. (2012). Performance of traffic networks during multimodal evacuations: Simulation-based assessment. *Natural Hazards Review*, 13(3), 196–204. [https://doi.org/10.1061/\(ASCE\)NH.1527-6996.0000065](https://doi.org/10.1061/(ASCE)NH.1527-6996.0000065)
- Peacock, R. D., Kuligowski, E. D., & Averill, J. D. (2011). *Pedestrian and evacuation dynamics*. Springer.
- Pipes, L. A. (1967). Car following models and the fundamental diagram of road traffic. *Transportation Research*, 1(1), 21–29. [https://doi.org/10.1016/0041-1647\(67\)90092-5](https://doi.org/10.1016/0041-1647(67)90092-5)
- Pursals, S. C., & Garzón, F. G. (2009). Optimal building evacuation time considering evacuation routes. *European Journal of Operational Research*, 192(2), 692–699. <https://doi.org/10.1016/j.ejor.2007.10.004>
- Saeed Osman, M., & Ram, B. (2017). Routing and scheduling on evacuation path networks using centralized hybrid approach. *Computers & Operations Research*, 88, 332–339. <https://doi.org/10.1016/j.cor.2017.06.022>
- Sarmady, S., Haron, F., & Talib, A. Z. (2011). A cellular automata model for circular movements of pedestrians during Tawaf. *Simulation Modelling Practice and Theory*, 19(3), 969–985. <https://doi.org/10.1016/j.simpat.2010.12.004>
- Sayyady, F., & Eksioğlu, S. D. (2010). Optimizing the use of public transit system during no-notice evacuation of urban areas. *Computers & Industrial Engineering*, 59(4), 488–495. <https://doi.org/10.1016/j.cie.2010.06.001>
- Shende, A. (2008). Optimization based nonlinear feedback control for pedestrian evacuation from a network of corridors [Doctor of Philosophy PhD thesis, Virginia Polytechnic Institute and State University, Blacksburg, VA]. <https://vtechworks.lib.vt.edu/handle/10919/30263>.
- Shende, A., Singh, M. P., & Kachroo, P. (2013). Optimal feedback flow rates for pedestrian evacuation in a network of corridors. *Transactions on Intelligent Transportation Systems*, 14(3), 1053–1066. <https://doi.org/10.1109/TITS.2013.2250965>
- Smith, J. M. (1991). State-dependent queueing models in emergency evacuation networks. *Transportation Research Part B: Methodological*, 25(6), 373–389. [https://doi.org/10.1016/0191-2615\(91\)90031-D](https://doi.org/10.1016/0191-2615(91)90031-D)
- Smith, J. M. (2001). Evacuation networks. In C. A. Floudas, & P. M. Pardalos (Eds.), *Encyclopedia of optimization* (pp. 576–584). Kluwer Academic.
- Smith, J. M. (2011). Optimal routing in closed queueing networks with state dependent queues. *INFOR: Information Systems and Operational Research*, 49(1), 45–62. <https://doi.org/10.3138/infor.49.1.045>
- Smith, J. M. (2012). Topological arrangements of M/G/c/K, M/G/c/c queues in transportation and material handling systems. *Computers & Operations Research*, 39(11), 2800–2819. <https://doi.org/10.1016/j.cor.2012.02.009>
- Smith, J. M., & Cruz, F. R. B. (2014). M/G/c/c state dependent travel time models and properties. *Physica A: Statistical Mechanics and its Applications*, 395, 560–579. <https://doi.org/10.1016/j.physa.2013.10.048>
- Smith, J. M., & Kerbache, L. (2011). State dependent models of material handling systems in closed queueing networks. *International Journal of Production Research*, 50(2), 1–24. <https://doi.org/10.1080/00207543.2010.535041>
- Stepanov, A., & Smith, J. M. (2009). Multi-objective evacuation routing in transportation networks. *European Journal of Operational Research*, 198(2), 435–446. <https://doi.org/10.1016/j.ejor.2008.08.025>
- Taneja, L., & Bolia, N. B. (2018). Network redesign for efficient crowd flow and evacuation. *Applied Mathematical Modelling*, 53, 251–266. <https://doi.org/10.1016/j.apm.2017.08.030>
- Togawa, K. (1955). *Study on fire escapes basing on the observation of multitude currents*. Building Research Institute, Ministry of Construction.
- Tregenza, P. (1976). *The design of interior circulation*. Van Nostrand Reinhold.
- Underwood, R. T. (1960). *Speed, volume and density relationships*. Bureau of Highway Traffic, Yale University.
- van Woensel, T., & Cruz, F. (2014). Optimal routing in general finite multi-server queueing networks. *PLoS ONE*, 9(7), 1–15. <https://doi.org/10.1371/journal.pone.0102075>
- Wang, H., Li, J., Chen, Q.-Y., & Ni, D. (2011). Logistic modeling of the equilibrium speed–density relationship. *Transportation Research Part A: Policy and Practice*, 45(6), 554–566. <https://doi.org/10.1016/j.tra.2011.03.010>
- Weiss, A., Williams, L., & Smith, J. M. (2012). Performance & optimization of M/G/c/c building evacuation networks. *Journal of Mathematical Modelling and Algorithms*, 11(4), 361–386. <https://doi.org/10.1007/s10852-012-9192-6>
- Yuhaski, S. J., & Smith, J. M. (1989). Modeling circulation systems in buildings using state dependent queueing models. *Queueing Systems*, 4(4), 319–338. <https://doi.org/10.1007/BF01159471>
- Zhang, Z., Jia, L., Qin, Y., & Yun, T. (2017). Optimization-based feedback control of passenger flow in subway stations for improving level of service. *Transportation Letters*, 11(8), 413–424. <https://doi.org/10.1080/19427867.2017.1374501>
- Zhang, Z., Jia, L., & Qin, Y. (2016). Level-of-service based hierarchical feedback control method of network-wide pedestrian flow. *Mathematical Problems in Engineering*, 2016, 1–14. <https://doi.org/10.1155/2016/9617890>
- Zhu, J., Hu, L., Jiang, Y., & Khattak, A. (2017). Circulation network design for urban rail transit station using a PH(n)/PH(n)/C/C queueing network model. *European Journal of Operational Research*, 260(3), 1043–1068. <https://doi.org/10.1016/j.ejor.2017.01.030>